Star-disc magnetospheric interaction and launching of outflows and jets

Miljenko Čemeljić

with W. Kluźniak,

V. Parthasarathy, A.D. Bollimpalli,

R. Mishra, A. Kotek

& summer students 2016, 2017 & 2018

Nicolaus Copernicus Astronomical Center,

Warsaw, Poland

& collaborators in ASIAA, Taiwan & CEA, France

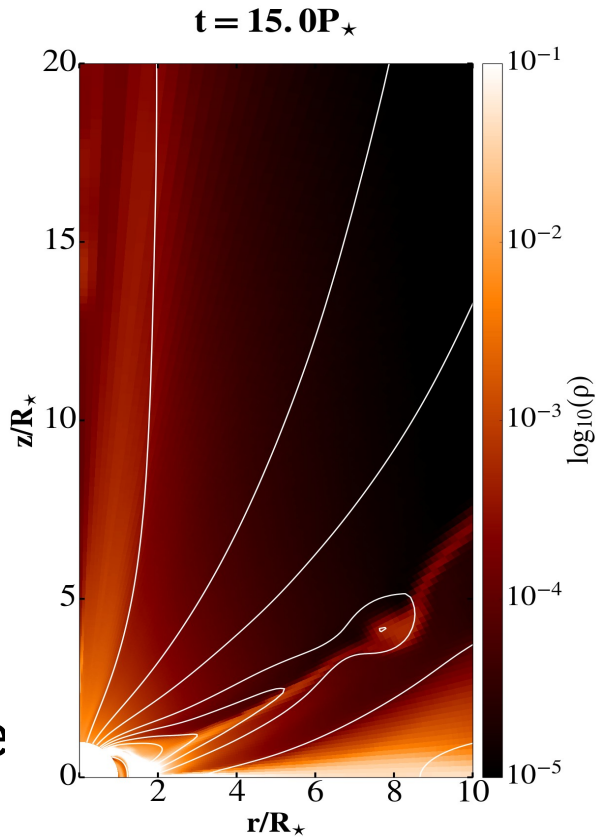

3D teaser

- From a 3D simulation one wishes to produce the synthetic maps, which could be compared with the observations. Here is a snapshot from my latest efforts on this. The dipole stellar magnetic field is tilted 45 deg with respect to the axis of rotation.

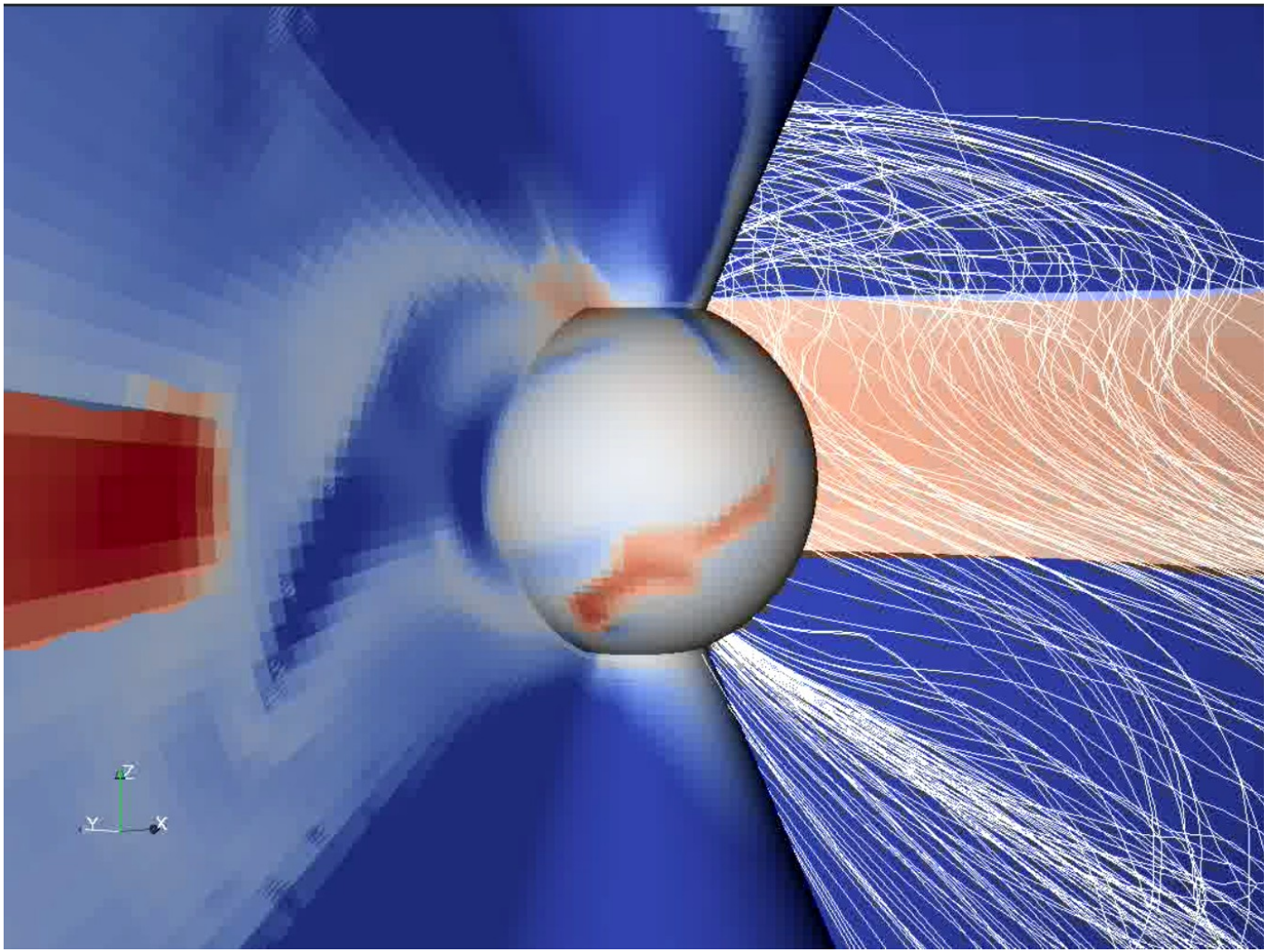

Outline

- 3D teaser
- Introduction - observations, theory
- Numerical simulations in HD and MHD
- “Atlas” of solutions
- Trends in the angular momentum flux
- Analytical equations for MHD disk and some solutions
- Case with backflow in the disk
- Outflows and jets launching
- 3D setup: HD, axisymmetric MHD & tilted mag.field
- Summary

Introduction-observations

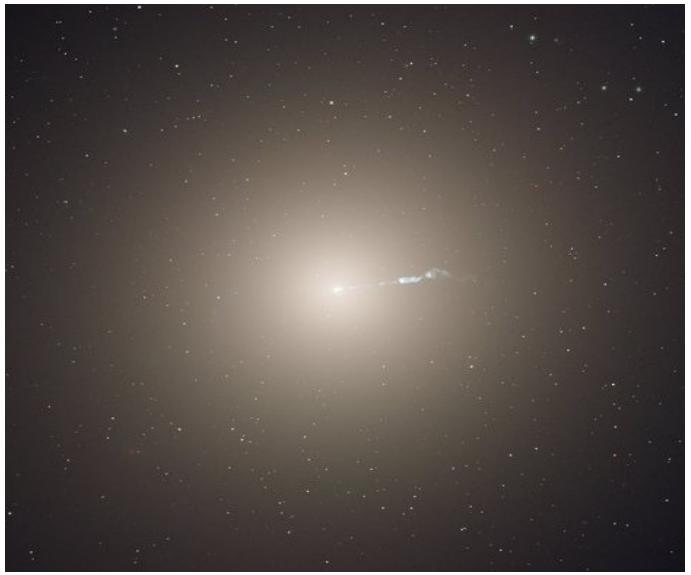

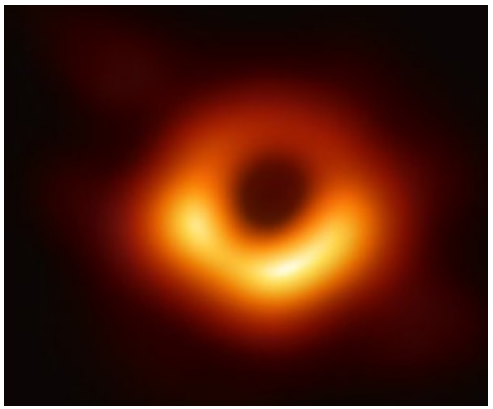

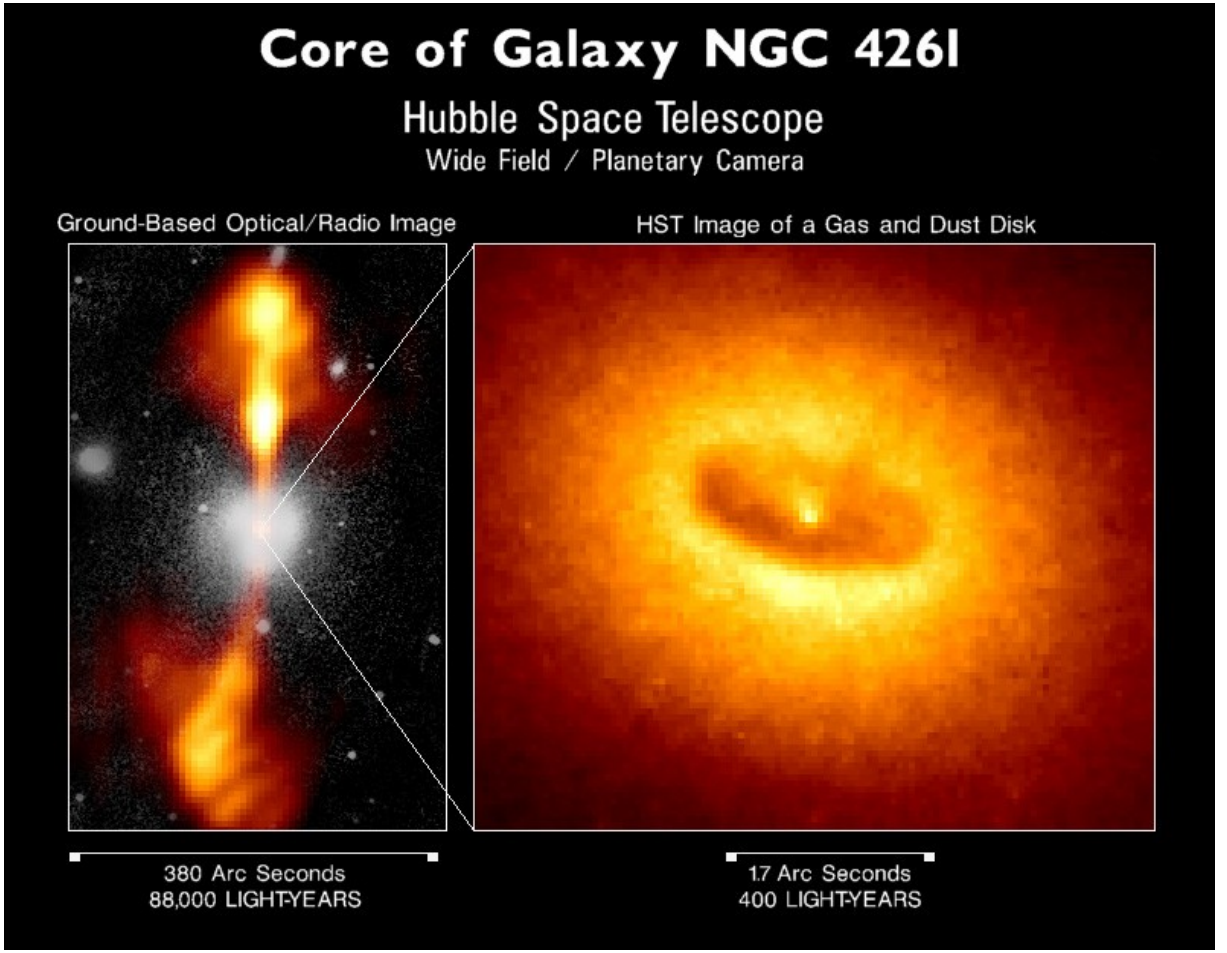

•We know about jets for more than 100 years -M87 was the first jet to be observed, by Curtis (1918). Only in the era of HST we obtained well resolved disk (dust and gas, not accretion disk!) and jet observations. In the case of M87 recently we got very, very close to the central BH.

Introduction-observations

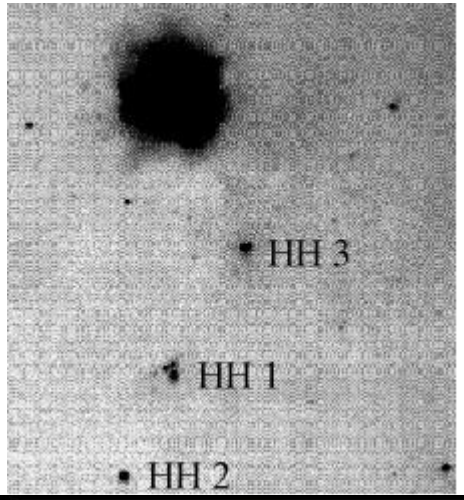

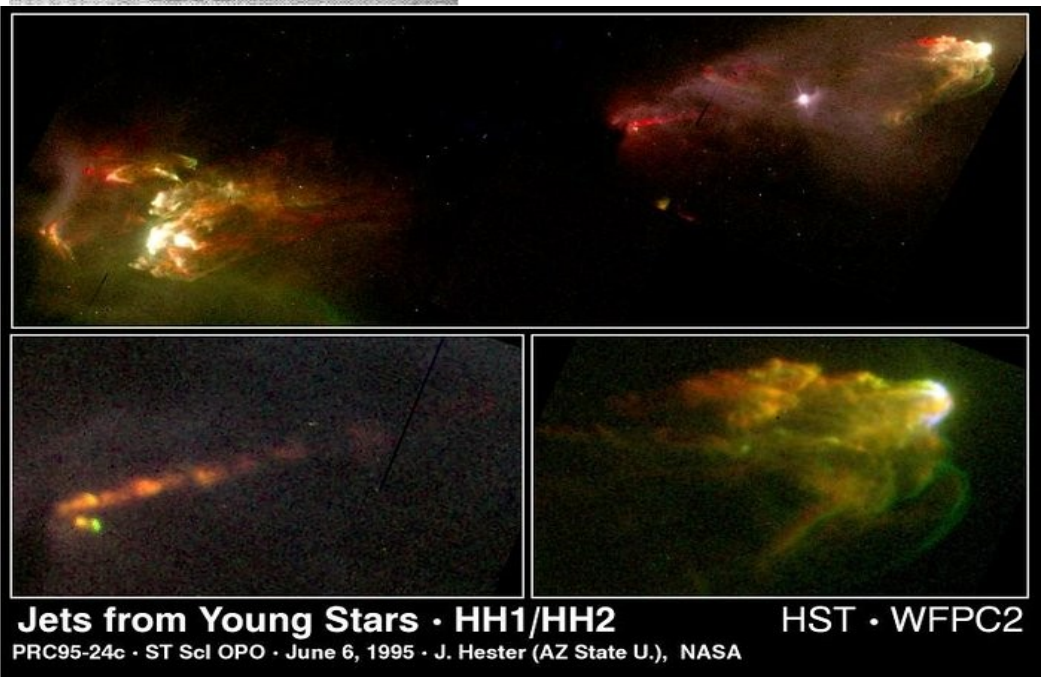

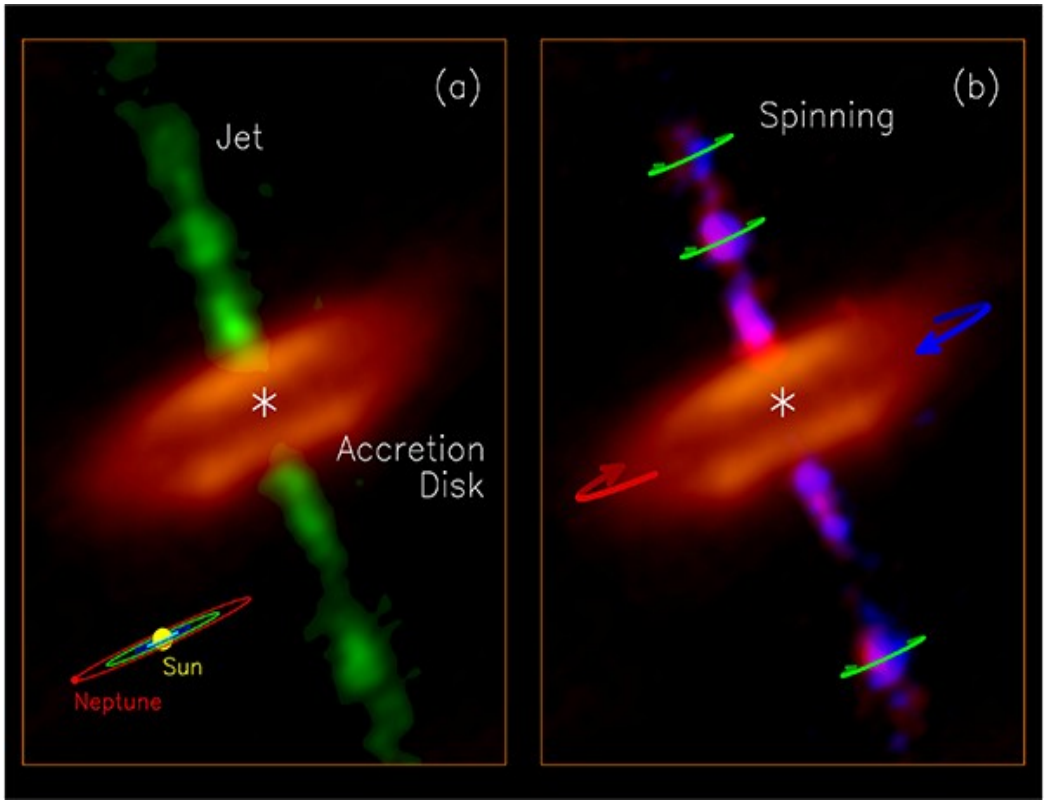

•Stellar jets followed in HH objects in 1950's. Here also only HST provided well resolved disk and jet observations. In the ALMA era, we got even closer-a team from ASIAA, Taiwan recently measured a rotating disk and jet in HH212. Resolution of the observation is down to 8 AU! The angular momentum carried by a jet is so small that it must be launched from the region well inside the disk, about 0.05 AU from the star. This matches with the magnetospheric jet launching.

Introduction-observations

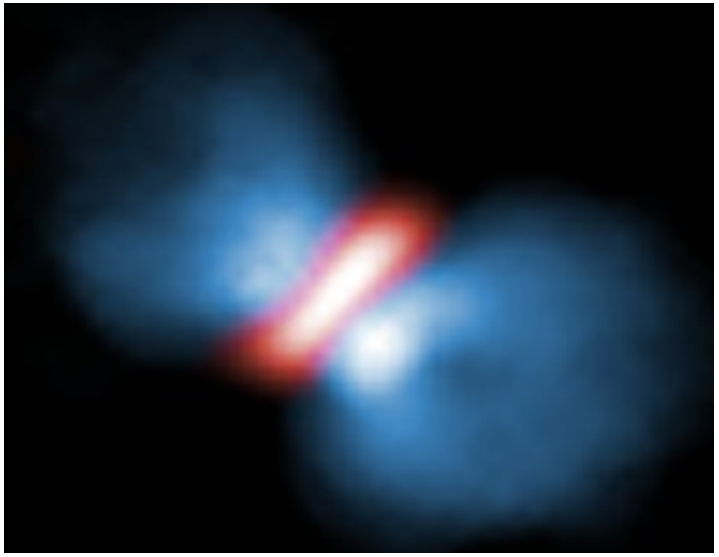

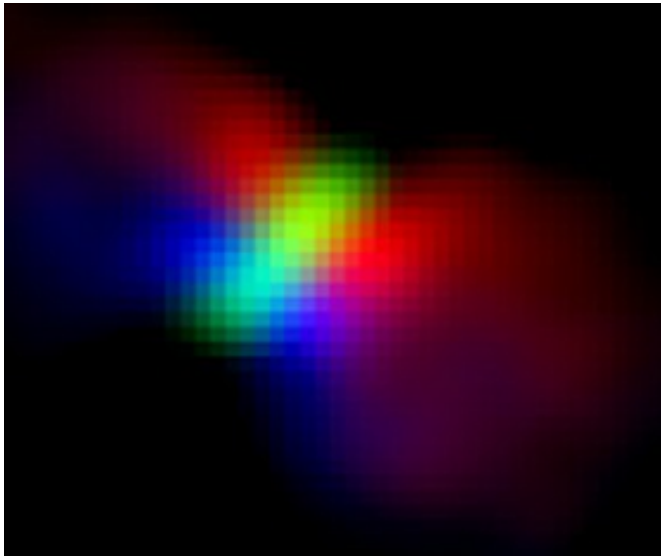

•Stellar outflows in the case of massive young stars comply more to the magnetocentrifugal outflow launching, where the outflow is launched from the disk surface. Here is a recent ALMA image for Orion KL Source 1, and measured velocities. In the right panel the color shows the motion of the gas: red shows gas moving away from us, blue shows gas moving toward us. The disk is shown in green (Hirota et al., 2017).

•Spectacular ALMA image of the HL Tau protoplanetary disk, with the planet trajectories carved-out, is another example of what we can expect from the new instruments (ALMA, 2014). A million years young star with a disk of more than three Neptune orbits radius, is located at 450 ly from us. It came as a large surprise that such a young star would already show signs of planet formation.

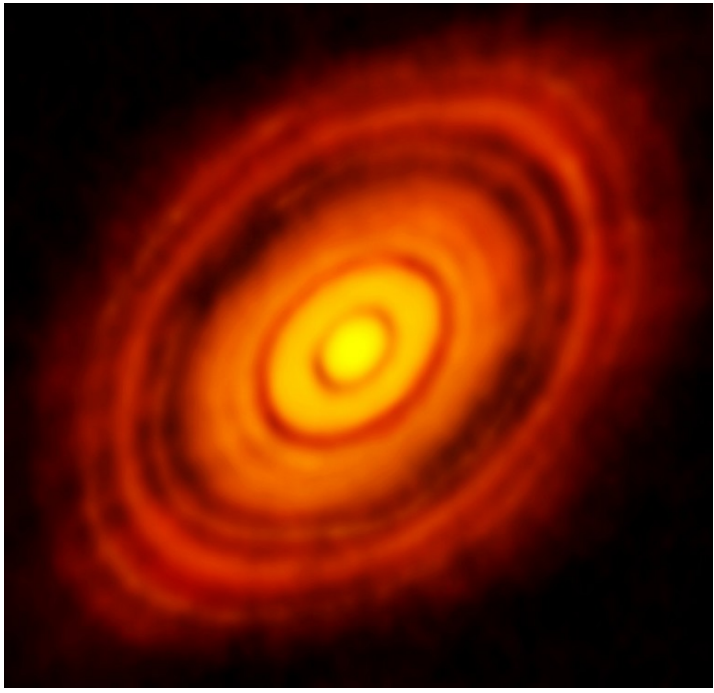

Introduction-theory

•First numerical solution of (HD) accretion disk was by Prendergast & Burbidge (1968)

•Analytical solution was given by Shakura & Sunyaev (1973)

• From that time to the 1990-ies many developments and models, with different approximations.

•In Kluźniak & Kita (2000, KK00) was given a solution of the HD disk in the full 3D. It was obtained by the method of asymptotic approximation.

•In 2009, numerical simulations of star-disk magnetospheric interaction were done in 2D-axisymmetric simulations, by Romanova et al. (2009, 2013, with non-public code), Zanni & Ferreira (2009, 2013, with publicly available code).

•Development of disk simulations in the direction of MRI in the disk (Flock et al.), but nothing much in star-disk magnetospheric simulations for a decade.

•In Čemeljić et al. (2017) and Čemeljić (2019), the first repeating of Zanni et al. (2009, 2013) axi-symmetric viscous & resistive MHD simulations in 2D with PLUTO code were reported. The results are similar to Romanova et al., obtained with their (non-public) code.

•A parameter study is now possible, to investigate the influence of different parameters-the beginning of this is published in Čemeljić (2019).

Equations for star-disk problem

•I perform simulations of thin accretion disk, which reach a quasi-stationary state.

•Ohmic and viscous heating in the energy equation are neglected, assuming that all the heat is radiated away.

•Viscosity and resistivity are still included, in the equation of motion and in the induction equation.

$$\frac{\partial \rho}{\partial t} + \nabla \cdot (\rho \boldsymbol{u}) = 0$$

$$\frac{\partial \rho \boldsymbol{u}}{\partial t} + \nabla \cdot \left[\rho \boldsymbol{u}\boldsymbol{u} + \left(P + \frac{\boldsymbol{B} \cdot \boldsymbol{B}}{8\pi} \right) \boldsymbol{I} - \frac{\boldsymbol{B}\boldsymbol{B}}{4\pi} - \boldsymbol{\tau} \right] = \rho \boldsymbol{g}$$

$$\frac{\partial E}{\partial t} + \nabla \cdot \left[\left(E + P + \frac{\boldsymbol{B} \cdot \boldsymbol{B}}{8\pi} \right) \boldsymbol{u} - \frac{(\boldsymbol{u} \cdot \boldsymbol{B})\, \boldsymbol{B}}{4\pi} \right]$$
$$+ \nabla \cdot [\eta_{\mathrm{m}} \boldsymbol{J} \times \boldsymbol{B}/4\pi - \boldsymbol{u} \cdot \boldsymbol{\tau}] = \rho \boldsymbol{g} \cdot \boldsymbol{u} - \Lambda_{\mathrm{cool}}$$

$$\frac{\partial \boldsymbol{B}}{\partial t} + \nabla \times (\boldsymbol{B} \times \boldsymbol{u} + \eta_{\mathrm{m}} \boldsymbol{J}) = 0.$$

•Code I use is PLUTO (v.4.1) by Mignone et al. (2007, 2012).

Star-disk simulations setup

- I add the stellar dipole field to the KK00 solution. Simulations with quadrupole, octupole and multipole field were also performed.
- Stellar surface is a rotating boundary around the origin of the spherical computational domain. We assume the star to be a (differentially) rotating magnetized rotator. The initial corona is a non-rotating corona in a hydrostatic balance.

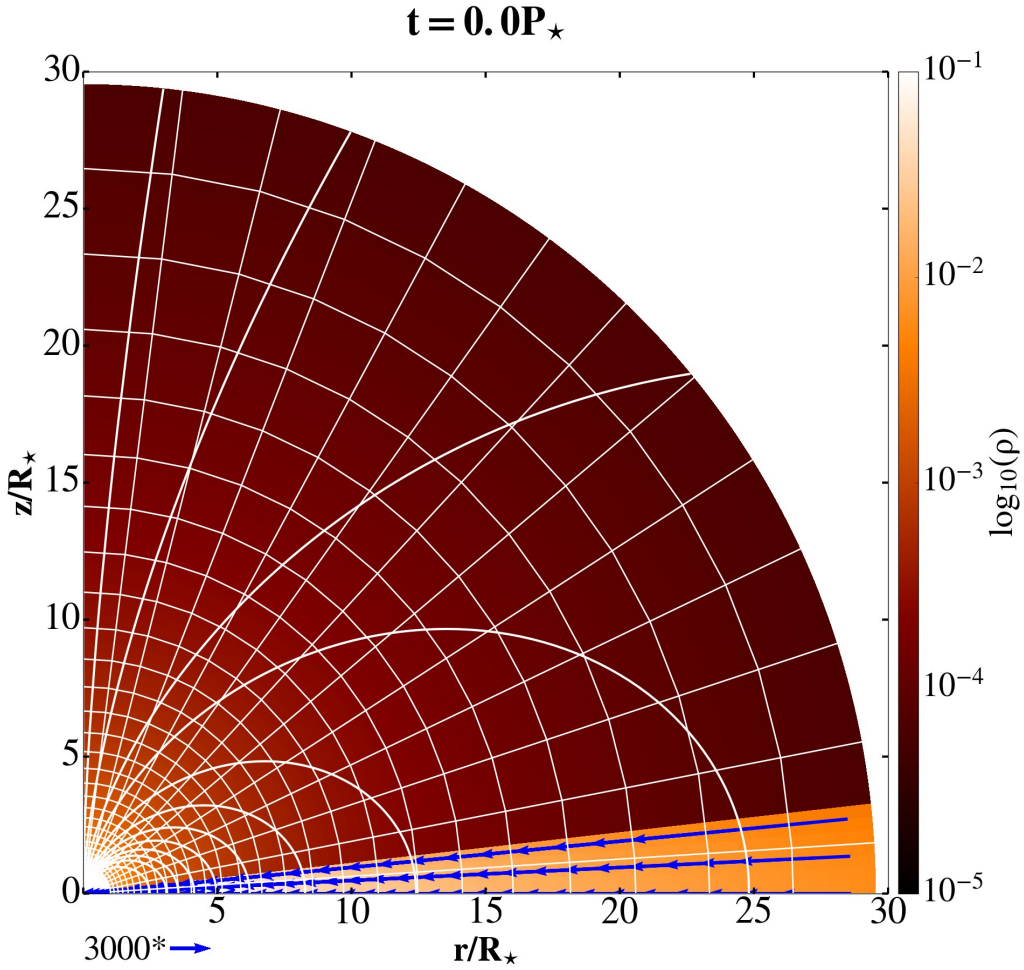

- In Čemeljić (2019) I performed a systematic study with magnetic star-disk numerical simulations, in 64 points in parameter space, for slow rotating star (up to 20% of the breakup velocity of the star). Cases with faster rotating star are currently investigated in work with R. Mishra and A. Kotek.

Star-disk simulations setup

- Resolution is Rxϑ=[217x100] grid cells in ϑ=[0,π/2], with a logarithmic grid spacing in the radial direction. The accretion column is well resolved.
- Star rotates at about 1/10 of the breakup rotational velocity.
- I did also Rxϑ=[217x200] grid cells in ϑ=[0,π] – I will show this later.

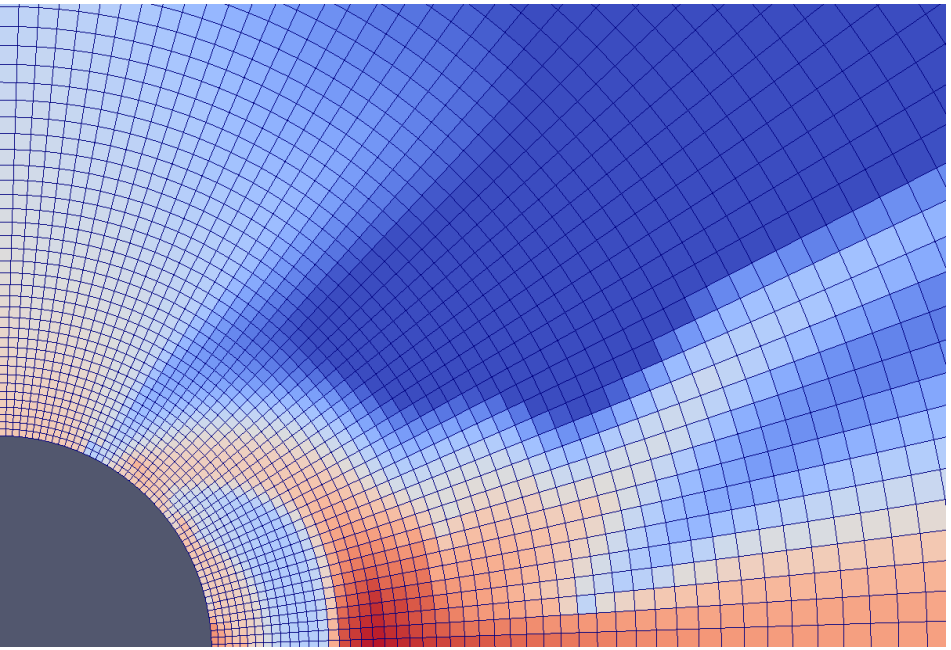

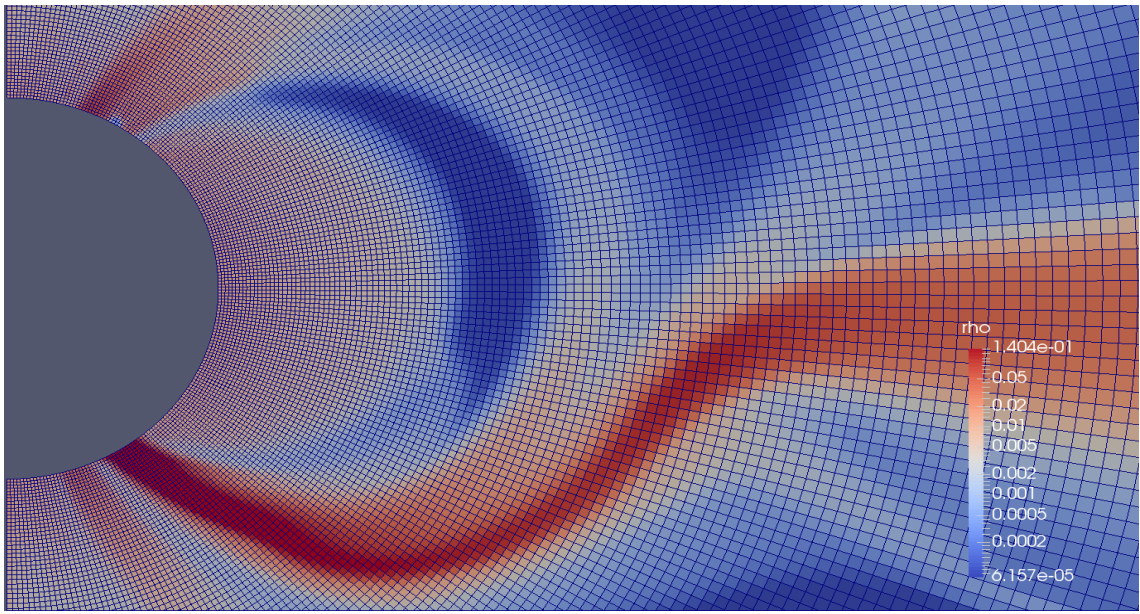

Hydro-dynamical star-disk simulations

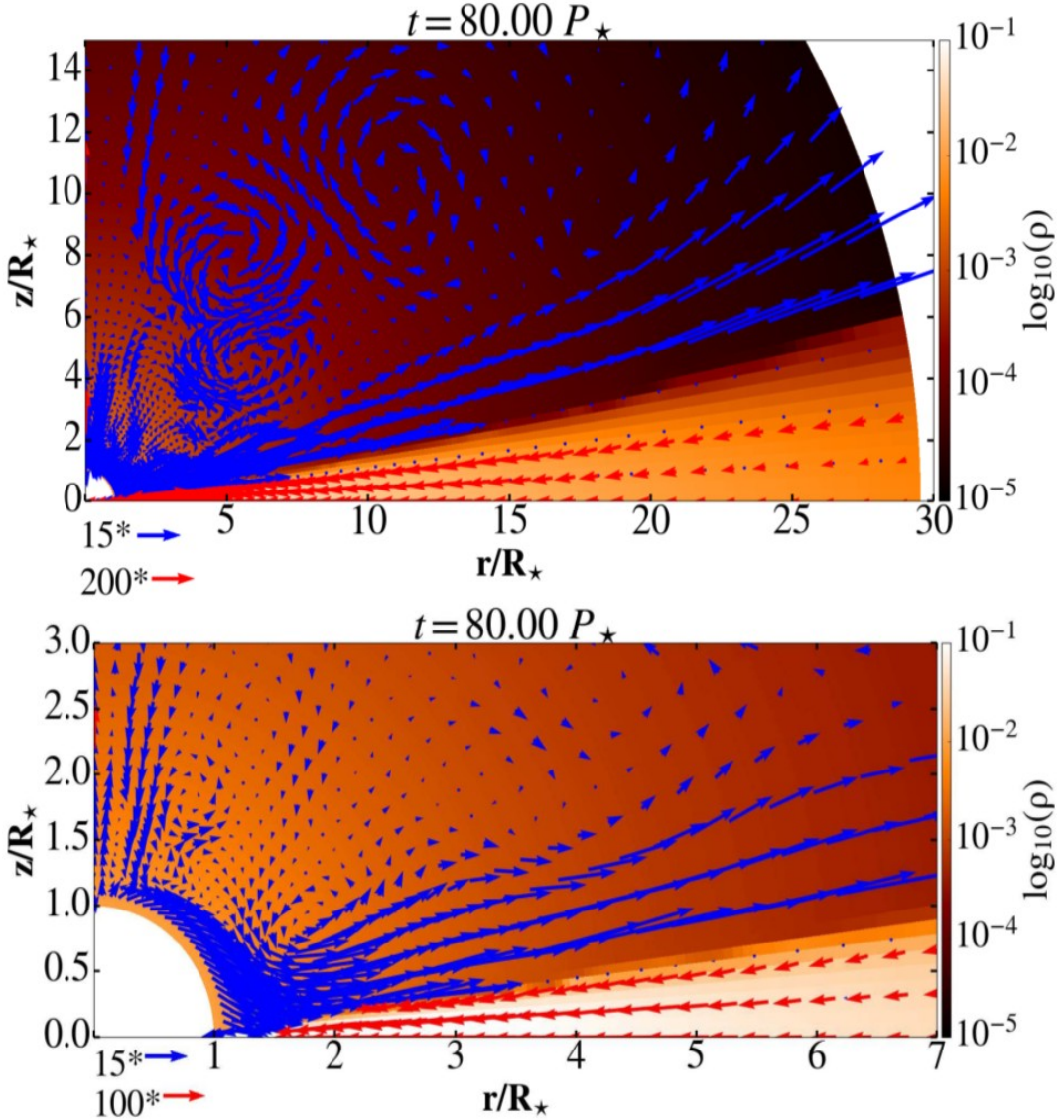

Computational box and a zoom closer to the star after 80 stellar rotations. In color is shown the density, and vectors show velocity, with the different normalization in the disk and stellar wind.

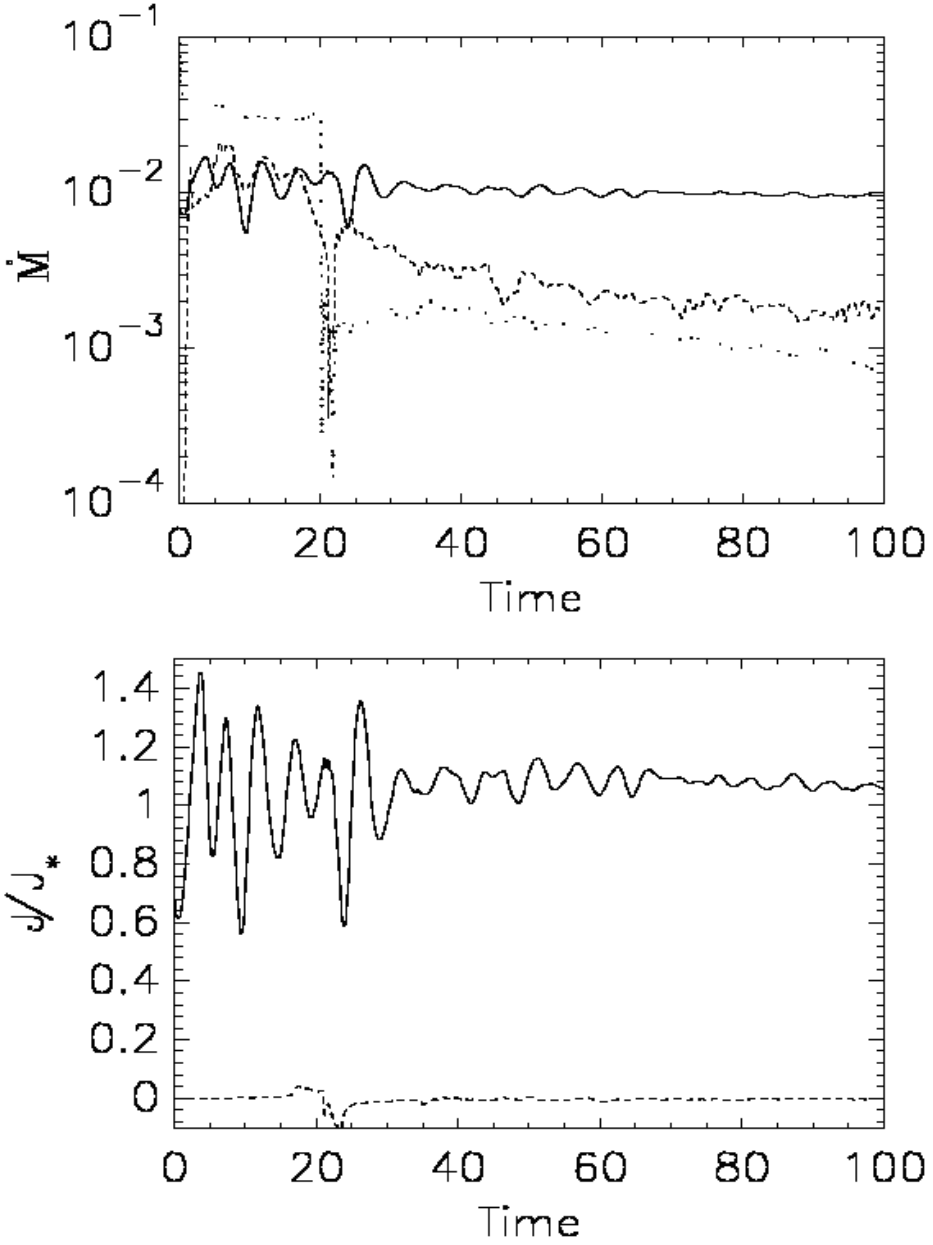

Time dependence of the mass and angular momentum fluxes in the various components in our simulations.

Star-disk magnetospheric interaction (SDMI) simulations

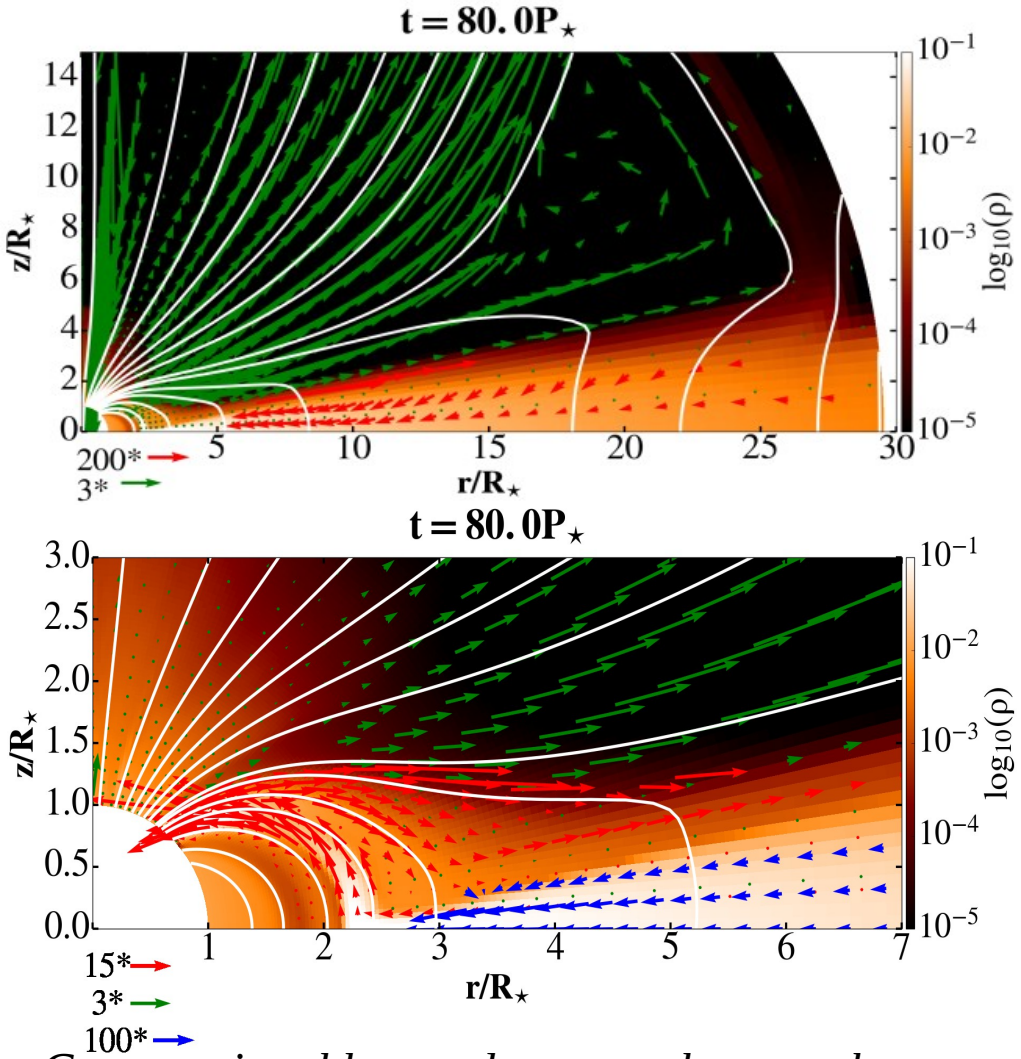

Computational box and a zoom closer to the star after 80 stellar rotations, to visualize the accretion column and the magnetic field lines (white solid lines) connected to the disk beyond the corotation radius Rcor=2.92 Rs. In color is shown the density, and vectors show velocity, with the different normalization in the disk, column and stellar wind.

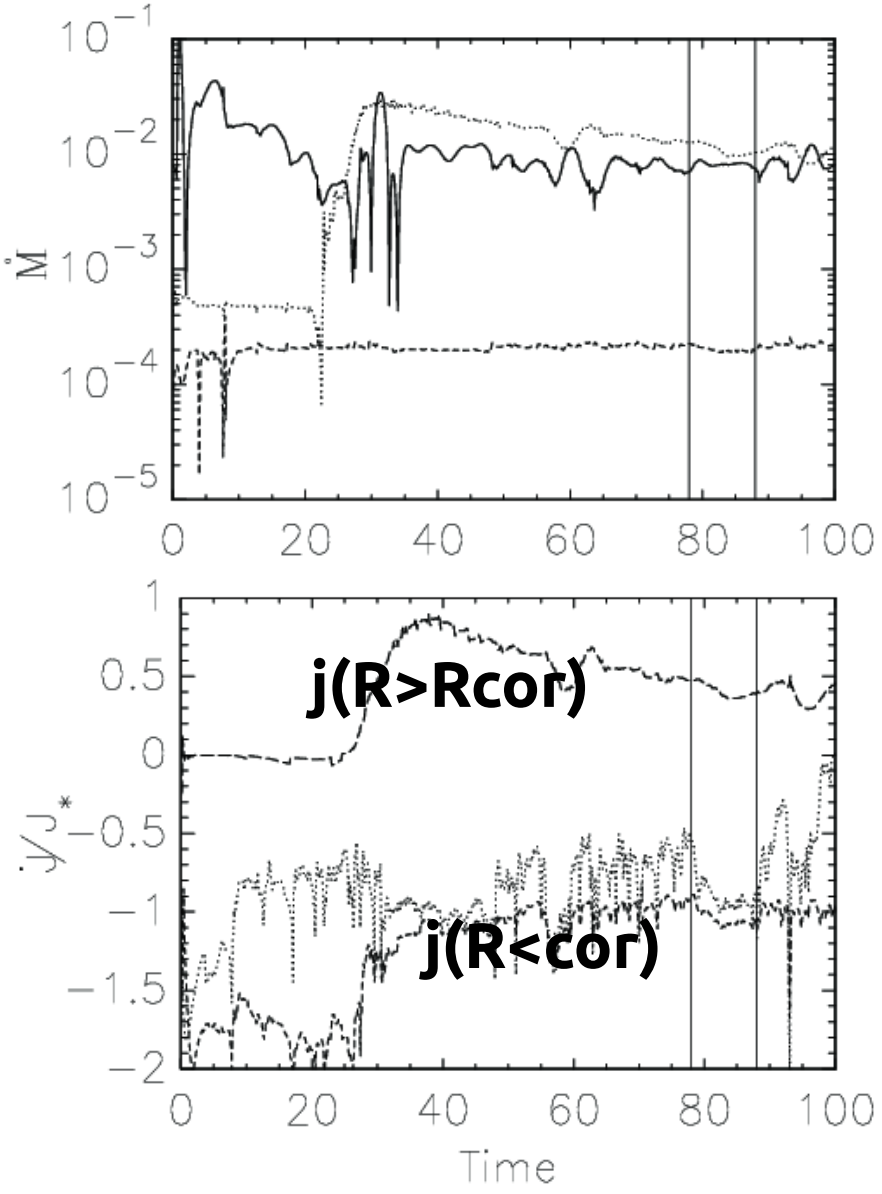

Time dependence of the mass and angular momentum fluxes in the various components in our simulations with marked the time interval in which the average for the quasi-stationarity is computed.

Part of the “Atlas” of solutions with different resistivities

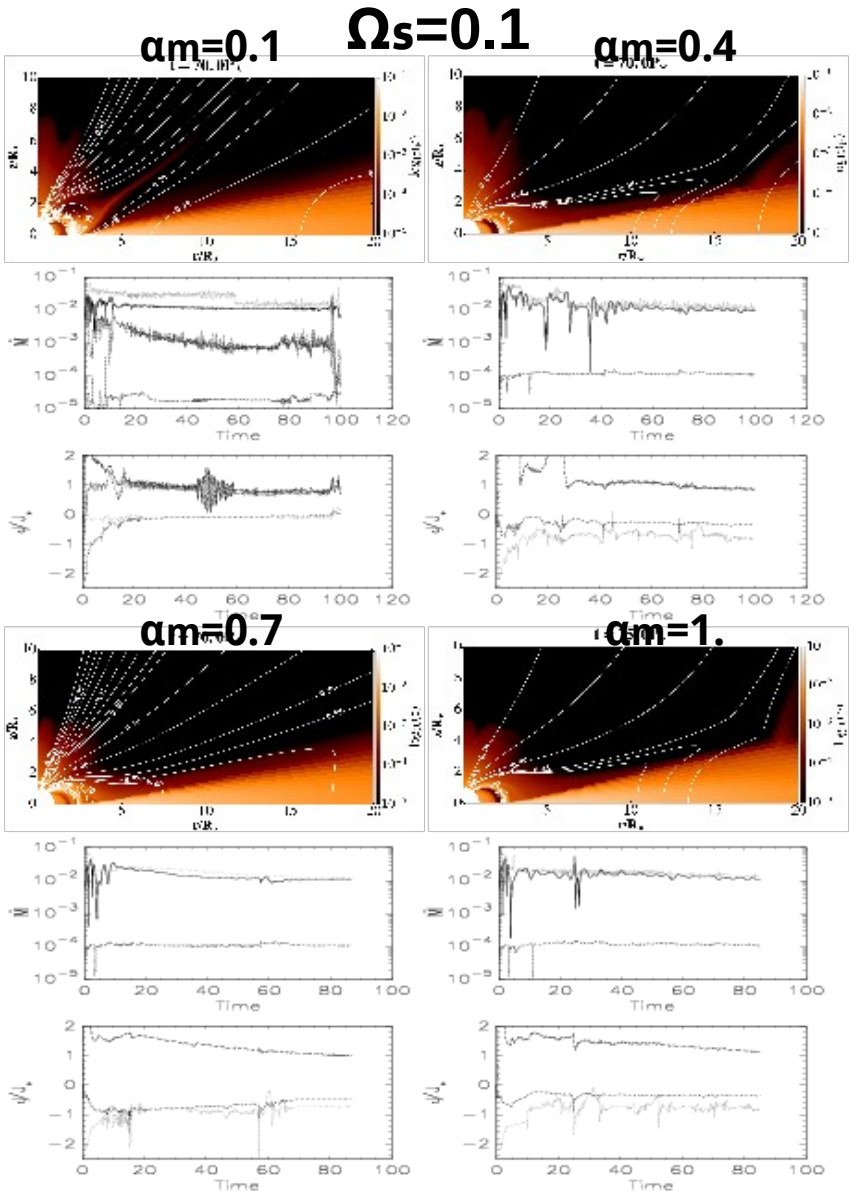

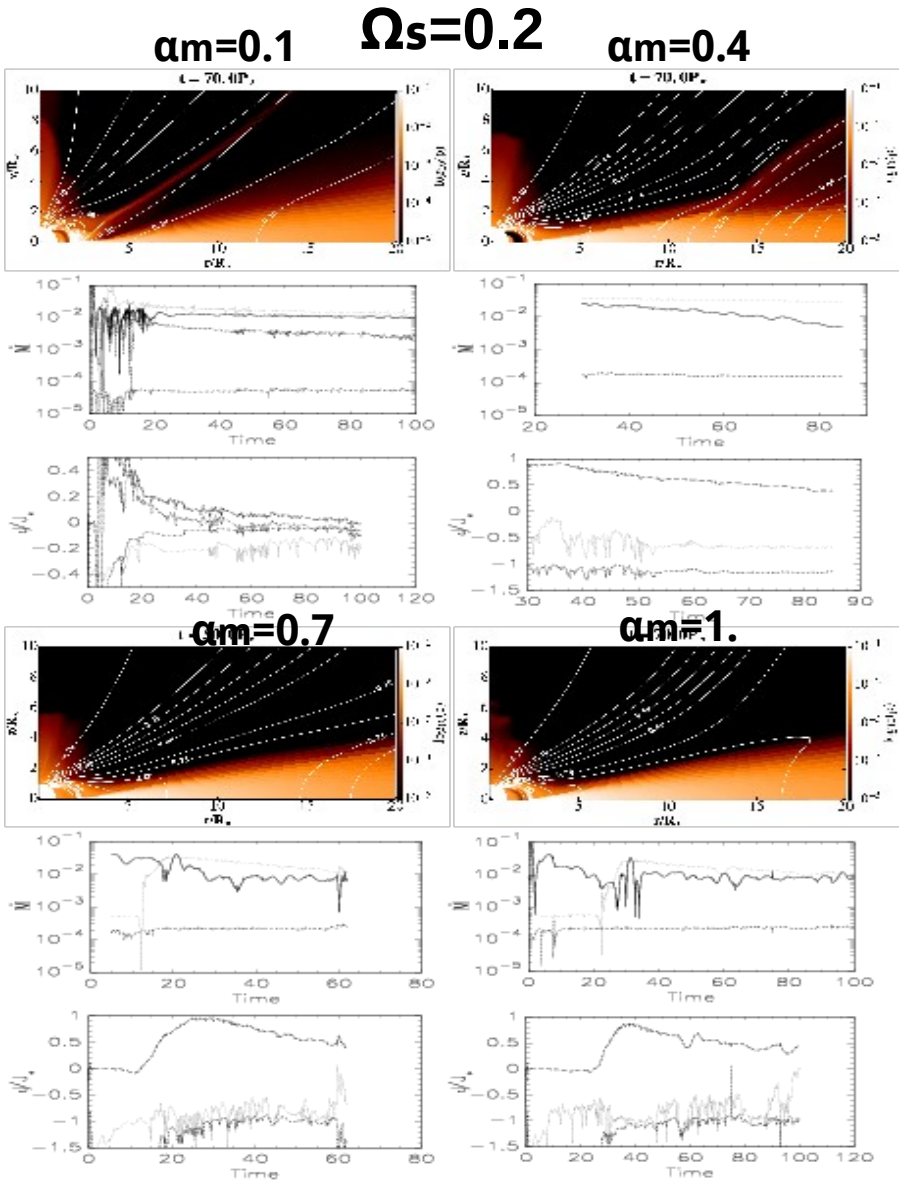

Configurations in “Atlas” solutions for slowly rotating stars

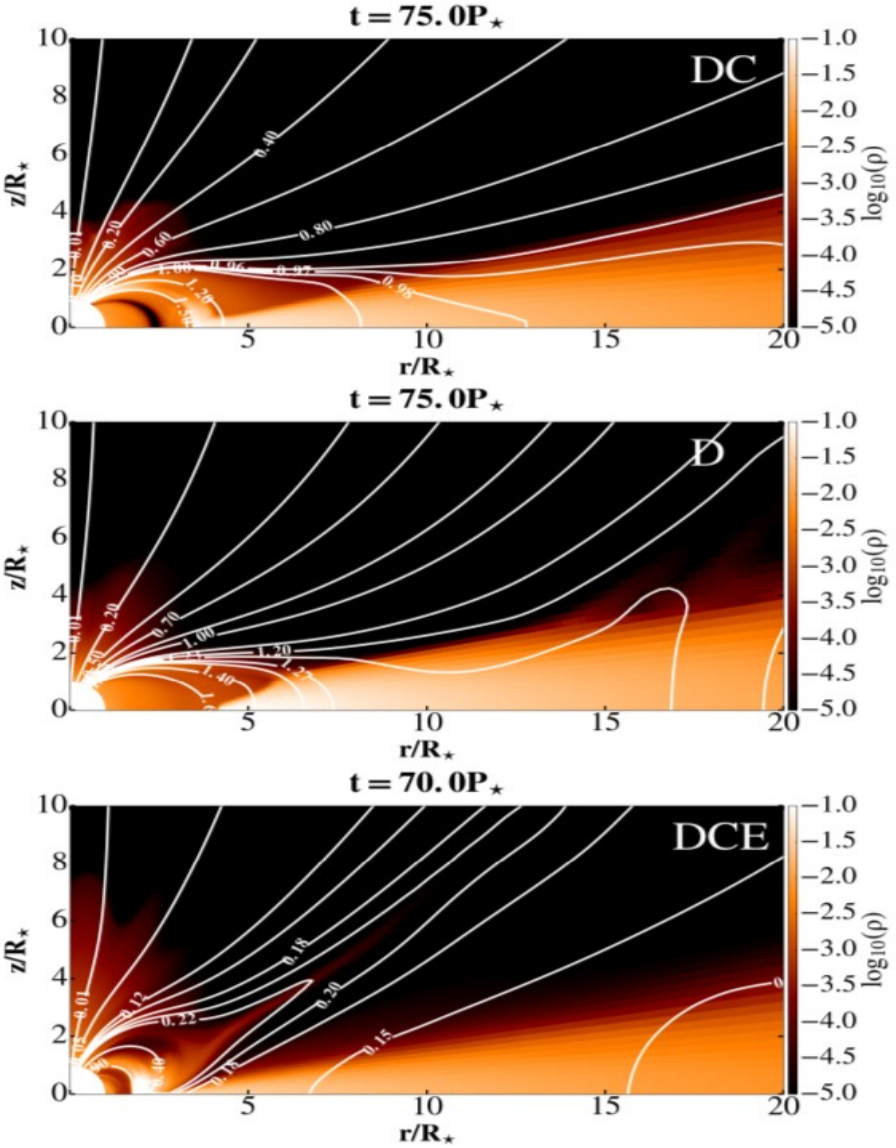

Three different cases of geometry in the results. In the top and middle panels are shown B=1 kG and the resistivity αm=1, in the cases with Ωs=0.1 (top panel) and Ωs=0.15 (middle panel). Faster stellar rotation prevents the accretion column formation. In the bottom panel is shown the third case, with B=0.5kG, resistivity αm=0.1 and Ωs=0.1, where a conical outflow is formed.

α_m =	0.1	0.4	0.7	1
$\Omega_\star/\Omega_{br}$				
		$B_\star$ = 250 G		
0.05	DCE	DC	DC	DC
0.1	DCE	DC	DC	DC
0.15	DCE	DC	DC	DC
0.2	DCE	DC	DC	DC
		$B_\star$ = 500 G		
0.05	DCE	DC	DC	DC
0.1	DCE	DC	DC	DC
0.15	DCE	DC	DC	DC
0.2	DCE	DC	DC	DC
		$B_\star$ = 750 G		
0.05	DCE	DC	DC	DC
0.1	DCE	DC	DC	DC
0.15	DCE	DC	DC	DC
0.2	DCE	DC	DC	DC
		$B_\star$ = 1000 G		
0.05	DCE	DC	DC	DC
0.1	DCE	DC	DC	DC
0.15	DCE	D	D	D
0.2	DCE	D	D	D

“Atlas” results: trends

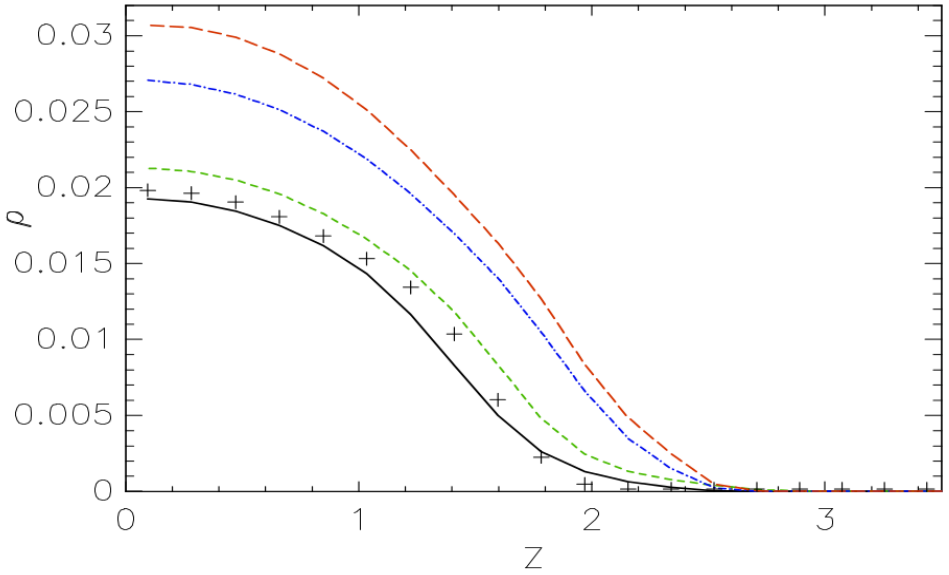

Fig. 3. Disk density in the simulations with $\Omega_\star = 0.2\Omega_{\rm br}$ and $\alpha_{\rm m} = 1$, measured along the disk height at $R = 12R_\star$. Results for $B_\star = 0.25$ (solid black line), 0.5 (short dashed green line), 0.75 (dash-dotted blue line) and 1 kG (long dashed red line) are shown. There is a trend in density with increasing stellar field. The result in the simulations without a magnetic field is shown with pluses.

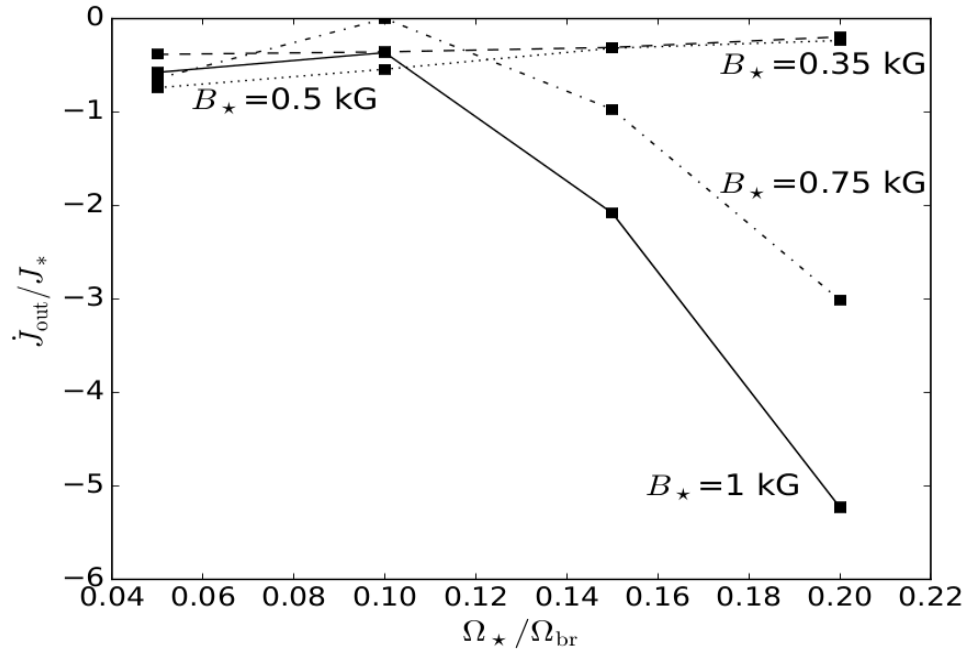

Fig. 5. Average angular momentum flux in the outflow that forms for $\alpha_{\rm m} = 0.1$. It is computed at $R = 12R_\star$ for different stellar rotation rates. Normalization is the same as in Fig. 4. Fluxes in $B_\star = 0.25$ (dotted), 0.5 (dash-dotted), 0.75 (dashed) and 1 kG (solid) are shown.

“Atlas” results: trends

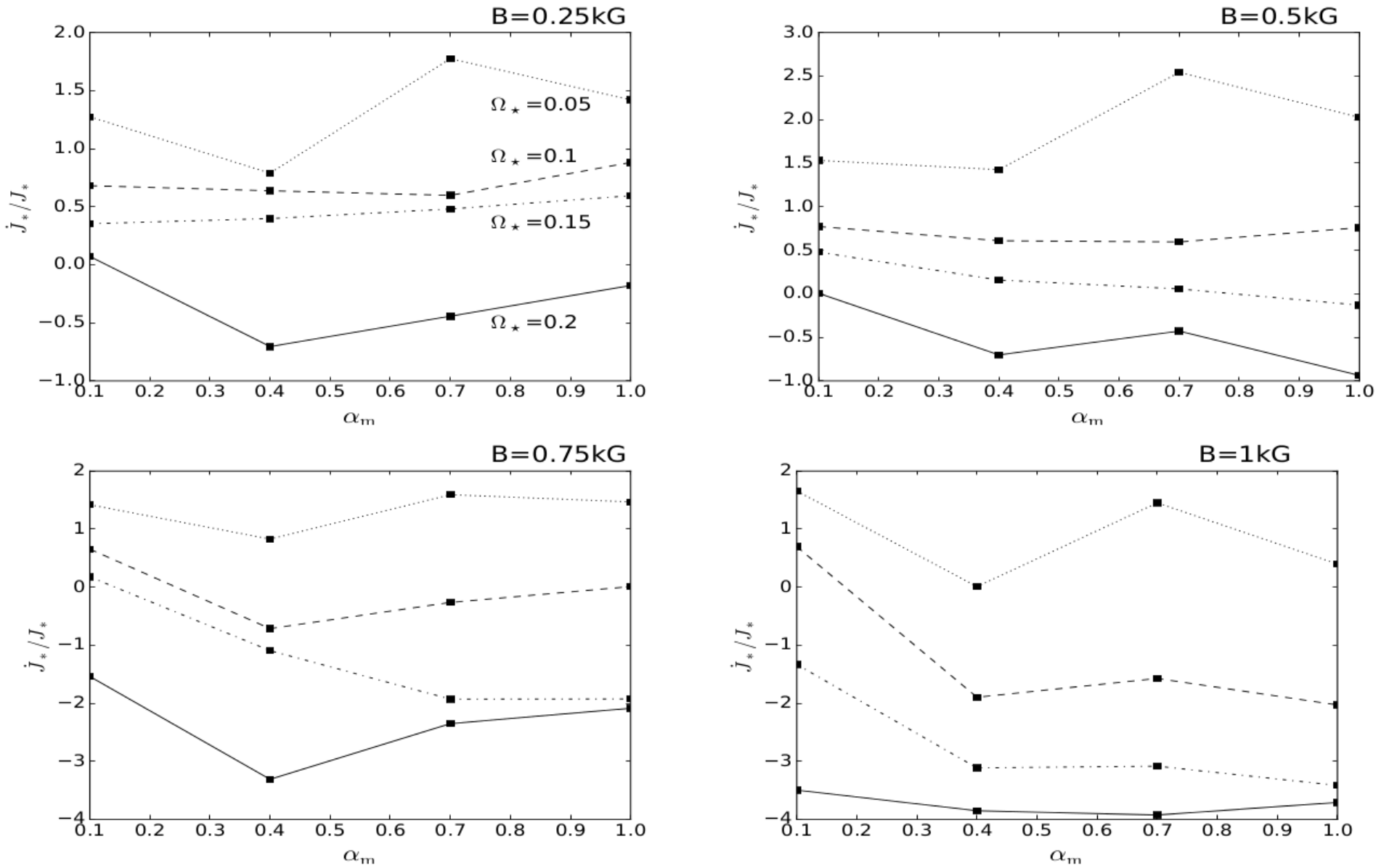

Fig. 4. Average angular momentum flux transported onto the stellar surface by the matter in-falling from the disk onto the star through the accretion column. Each panel shows a set of solutions with one stellar magnetic field strength and varying stellar rotation rate and resistivity. Results with $\Omega_\star/\Omega_{\rm br} = 0.05$ (dotted), 0.1 (dashed), 0.15 (dash-dot-dotted), and 0.2 (solid) are shown in units of stellar angular momentum $J_\star = k^2 M_\star R_\star^2 \Omega_\star$ (with $k^2 = 0.2$ for the typical normalized gyration radius of a fully convective star). A positive flux spins the star up, a negative flux slows it down. With the increase in stellar rotation rate, spin-up of the star by the infalling matter decreases and eventually switches to spin-down.

Analytical equations of the magnetized thin accretion disk-with WK and VP

In the asymptotic approximation, we write all the variables in the Taylor expansion with the coefficient of expansion $\epsilon = \tilde{H}/\tilde{R} << 1$ (see KK00). For a variable X, we then have $X = X_0 + \epsilon X_1 + \epsilon^2 X_2 + \epsilon^3 X_3 + \ldots$, and we can compare the terms of the same order in ϵ. Omitting primes in the normalized variables, we write the normalized equations of continuity, magnetic field solenoidality ($\nabla \cdot \boldsymbol{B} = 0$), momentum, induction and energy density.

Example: continuum eq., stationary state

$$\frac{\epsilon}{r}\partial_r[r(\rho_0 + \epsilon\rho_1 + \epsilon^2\rho_2 + \ldots)(v_{r0} + \epsilon v_{r1} + \epsilon^2\rho_2 + \ldots)]$$

$$+\partial_z[(\rho_0 + \epsilon\rho_1 + \epsilon^2\rho_2 + \ldots)(v_{z0} + \epsilon v_{z1} + \epsilon^2 v_{z2} + \ldots)] = 0.$$

From this we can write the term in the order zeroth order in ϵ as:

$$\frac{\partial}{\partial z}(\rho_0 v_{z0}) = 0 \;\Rightarrow v_{z0} = 0.$$

Since $\rho_0 \neq 0$, and v_z is odd with respect to z, at the disk equatorial plane it is $\rho_0 v_{z0} = 0$. Since it does not depend on z, we conclude that it must be $v_{z0} = 0$.

Comparison of results with increasing mag. field

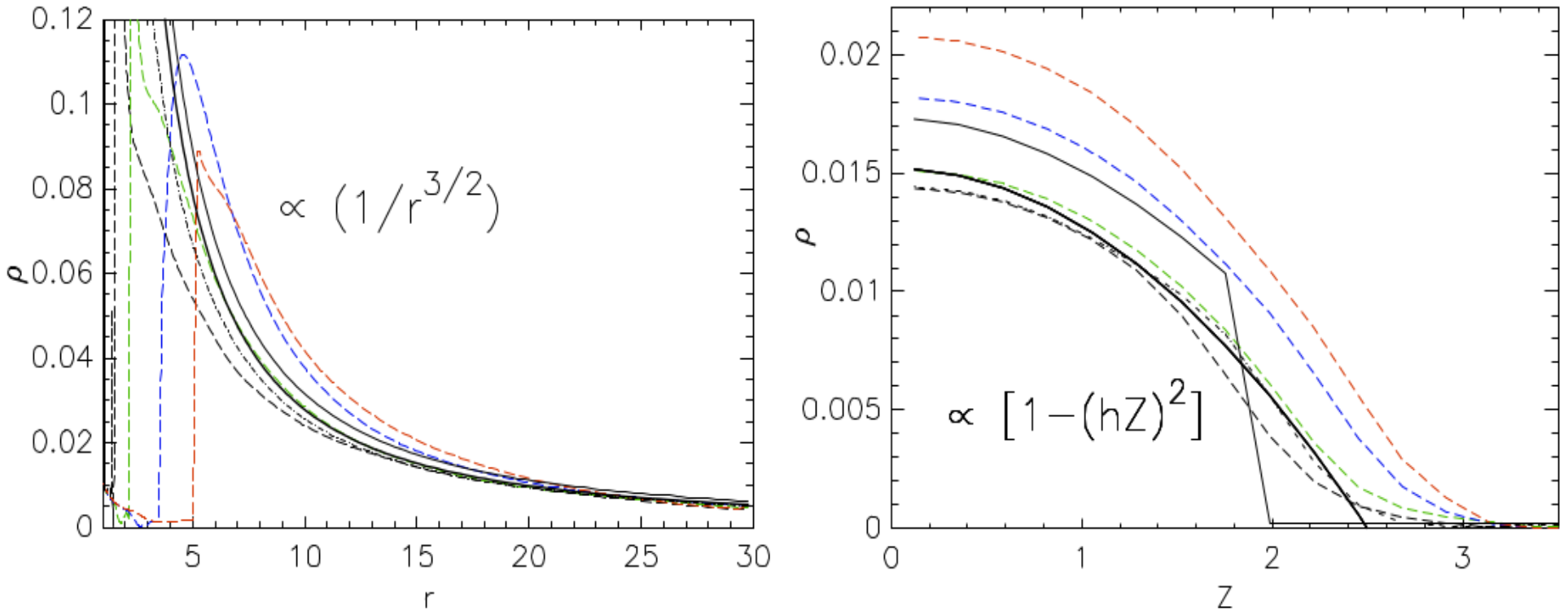

Comparison of the matter density in the initial set-up (thin solid line) with the quasi-stationary solutions in the numerical simulations in the HD (dot-dashed line) and the MHD (long-dashed line) cases. In black, green blue and red colors are the results in the MHD cases with the stellar magnetic field strength 0.25, 0.5, 0.75 and 1.0 kG, respectively. The closest match to the 0.5 kG case is depicted with the thick solid line. In the left panel is shown the radial dependence nearby the disk equatorial plane, and in the right panel the profiles along the vertical line at r=15.

Comparison of results with increasing mag. field

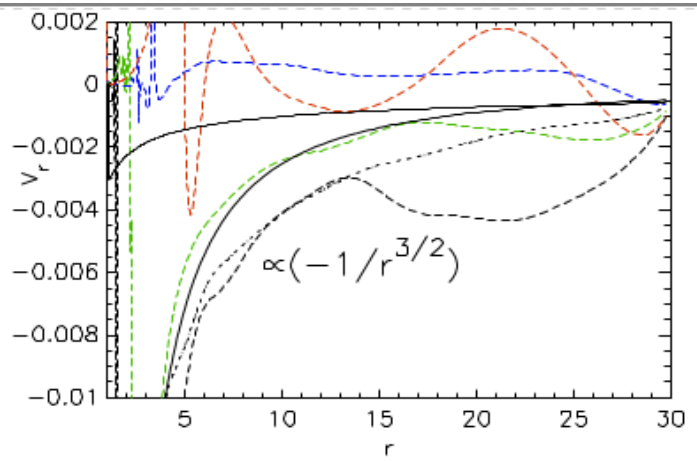

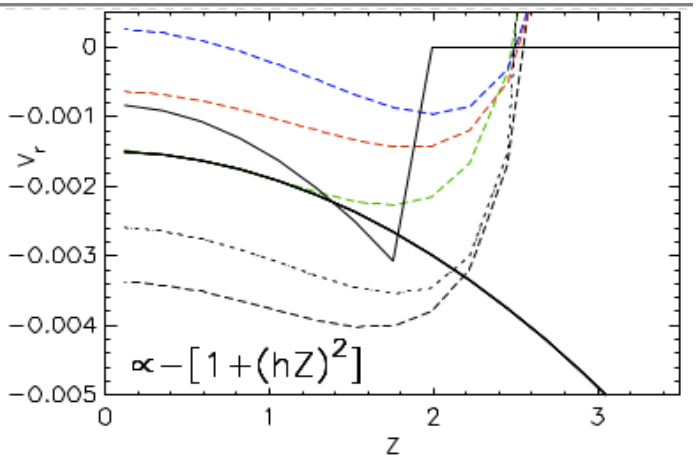

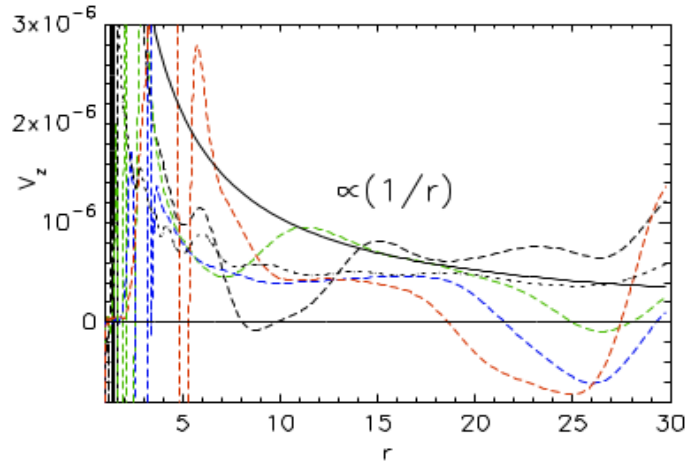

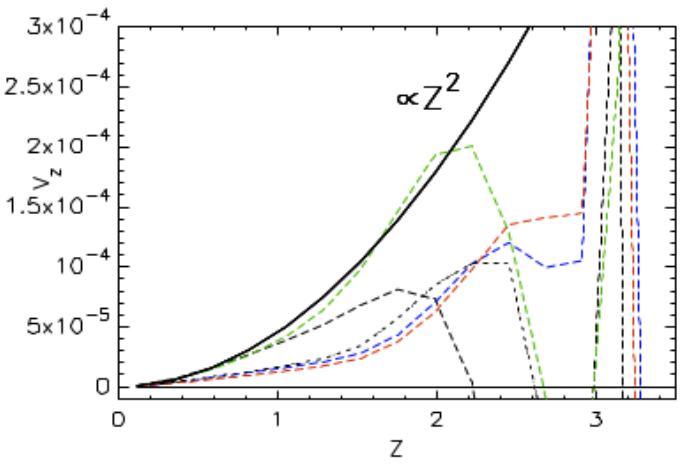

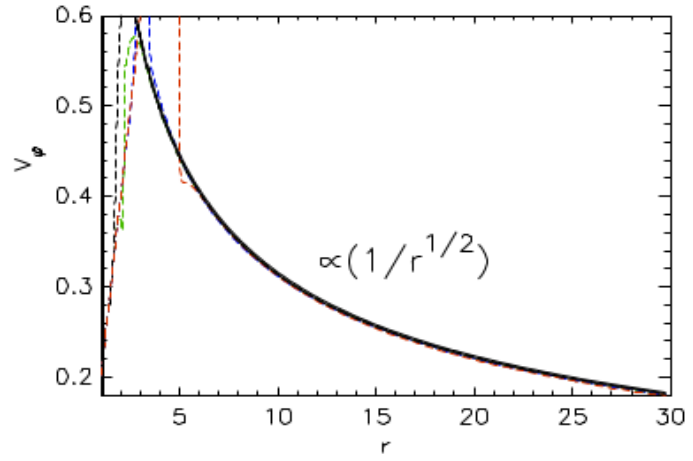

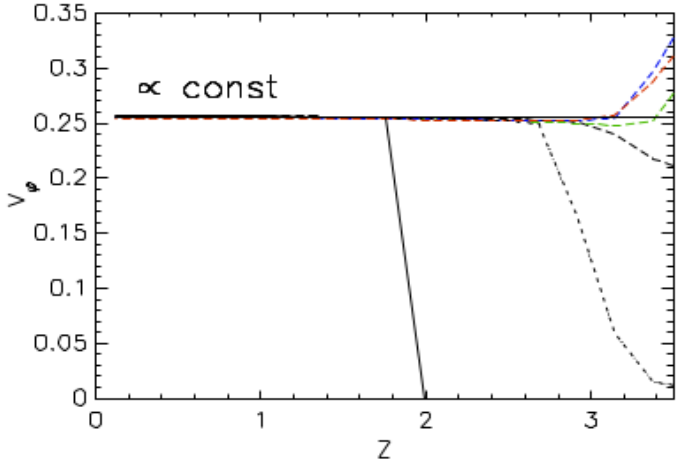

Comparison for velocities. In black, green blue and red colors are the results in the MHD cases with the stellar magnetic field strength 0.25, 0.5, 0.75 and 1.0 kG, respectively. The closest match to the 0.5 kG case is depicted with the thick solid line.

Comparison of results with increasing mag. field

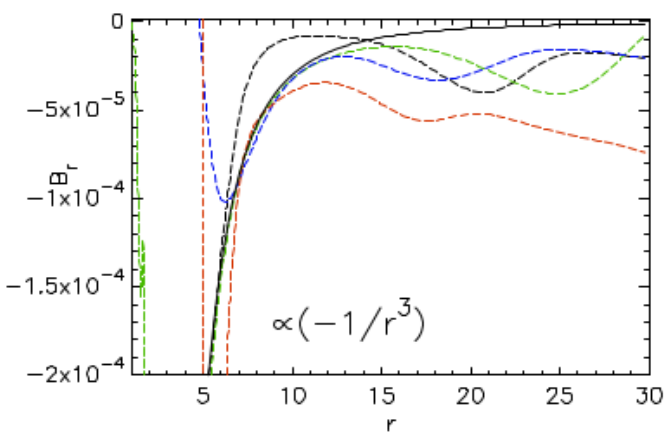

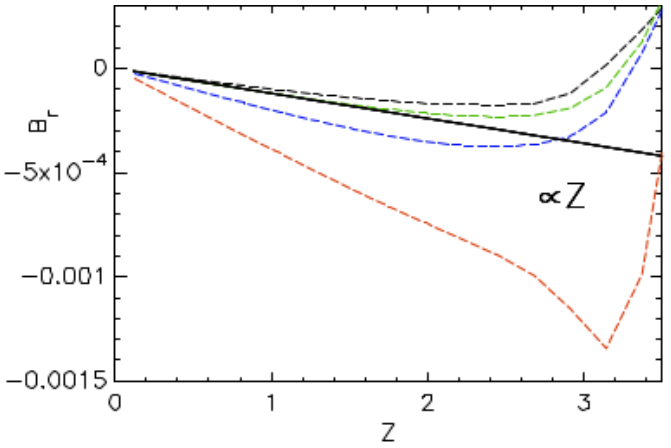

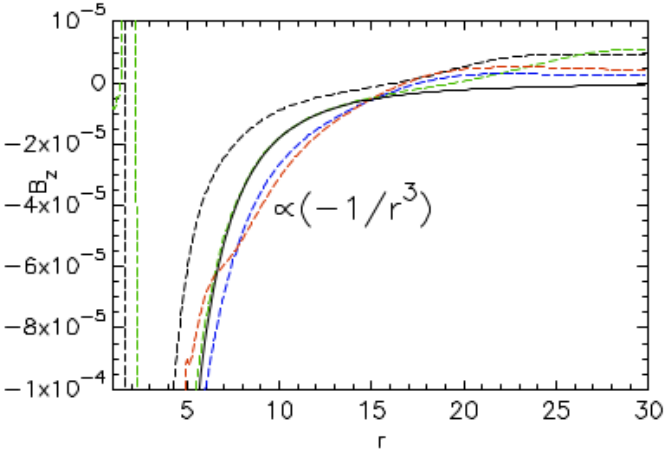

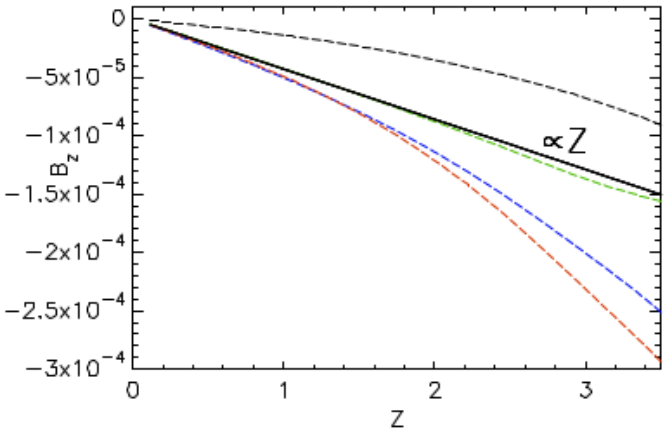

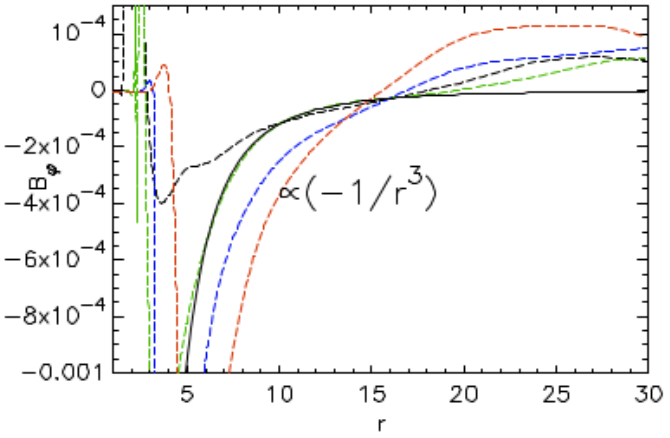

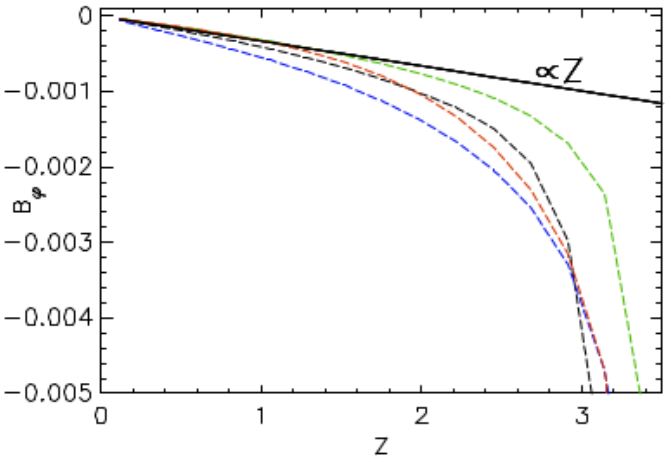

Comparison for magnetic field. In black, green blue and red colors are the results in the MHD cases with the stellar magnetic field strength 0.25, 0.5, 0.75 and 1.0 kG, respectively.

The closest match to the 0.5 kG case is depicted with the thick solid line.

Comparison of results with increasing mag. field

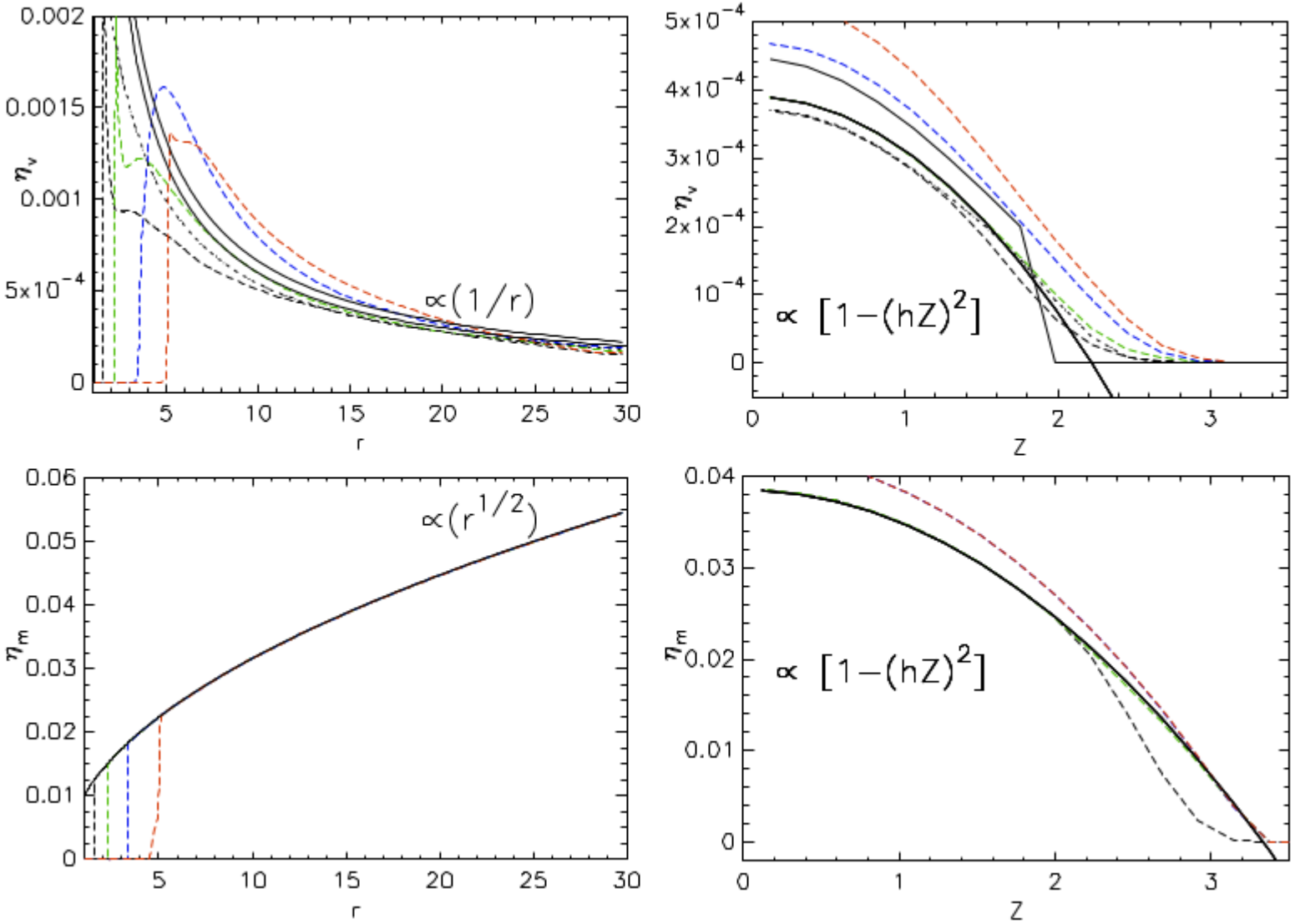

Comparison for viscosity and resistivity. In black, green blue and red colors are the results in the MHD cases with the stellar magnetic field strength 0.25, 0.5, 0.75 and 1.0 kG, respectively. The closest match to the 0.5 kG case is depicted with the thick solid line.

Comparison of results with increasing mag. field

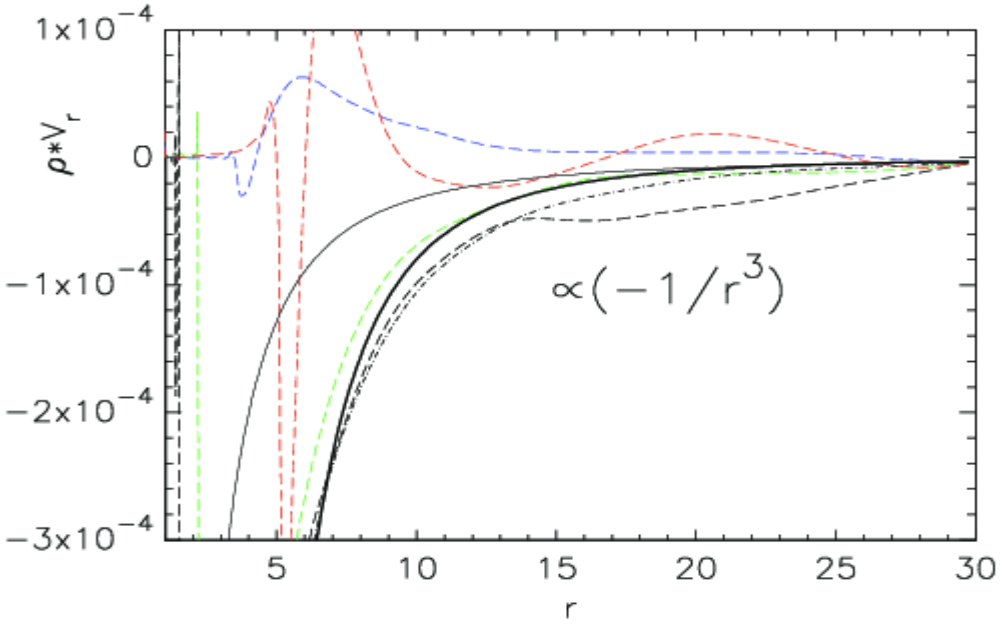

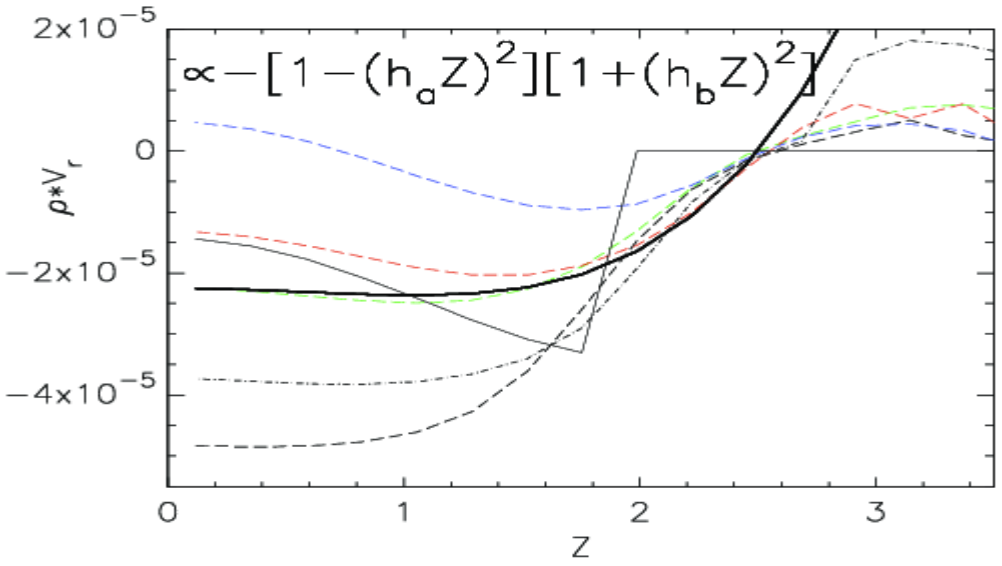

Comparison for the radial momentum. In black, green blue and red colors are the results in the MHD cases with the stellar magnetic field strength 0.25, 0.5, 0.75 and 1.0 kG, respectively. The closest match to the 0.5 kG case is depicted with the thick solid line.

Analytical expressions for magnetic disk solutions

- *Eqs of thin MHD disk can not be solved without knowing the solution at the disk surface, so we combine the analytical and numerical results to see if the analytical conditions are satisfied in the simulations.*

$$\rho(r,z) = \frac{k_1}{r^{3/2}}[1-(0.4z)^2],$$

$$v_r(r,z) = \frac{k_2}{r^{3/2}}[1+(0.5z)^2],\ v_z(r,z) = \frac{k_3}{r}z^{3/2},\ v_\varphi(r,z) = \frac{k_4}{\sqrt{r}},$$

$$B_r(r,z) = \frac{k_5}{r^3}z,\ B_z(r,z) = \frac{k_6}{r^3}z,\ B_\varphi(r,z) = \frac{k_7}{r^3}z,$$

$$\eta(r,z) = \frac{k_8}{r}[1-(0.45z)^2],\ \eta_{\rm m}(r,z) = k_9\sqrt{r}[1-(0.3z)^2].$$

Expressions for the physical quantities in the disk. k are the proportionality factors of matching curves.

k_1	k_2	k_3	k_4	k_5	k_6	k_7	k_8	k_9
0.88	-0.09	3.8×10^{-5}	0.255	-0.4	-0.15	-1.11	0.006	0.01

Proportionality coefficients in expressions at R=15Rs for the physical quantities in the disk,with Bs=500 G.

Backflows in the disk – HD case (with R. Mishra)

- Backflows in the disk occur in a portion of the parameter space. They were oberved in the earlier simulations by….. In Zanni & Ferreira (2009) it was commented that the origin of the outflow in the simulations is “numerical”. But, in KK00 analytical solutions they are present in the cases with the viscosity parameter alpha_v<0.685.

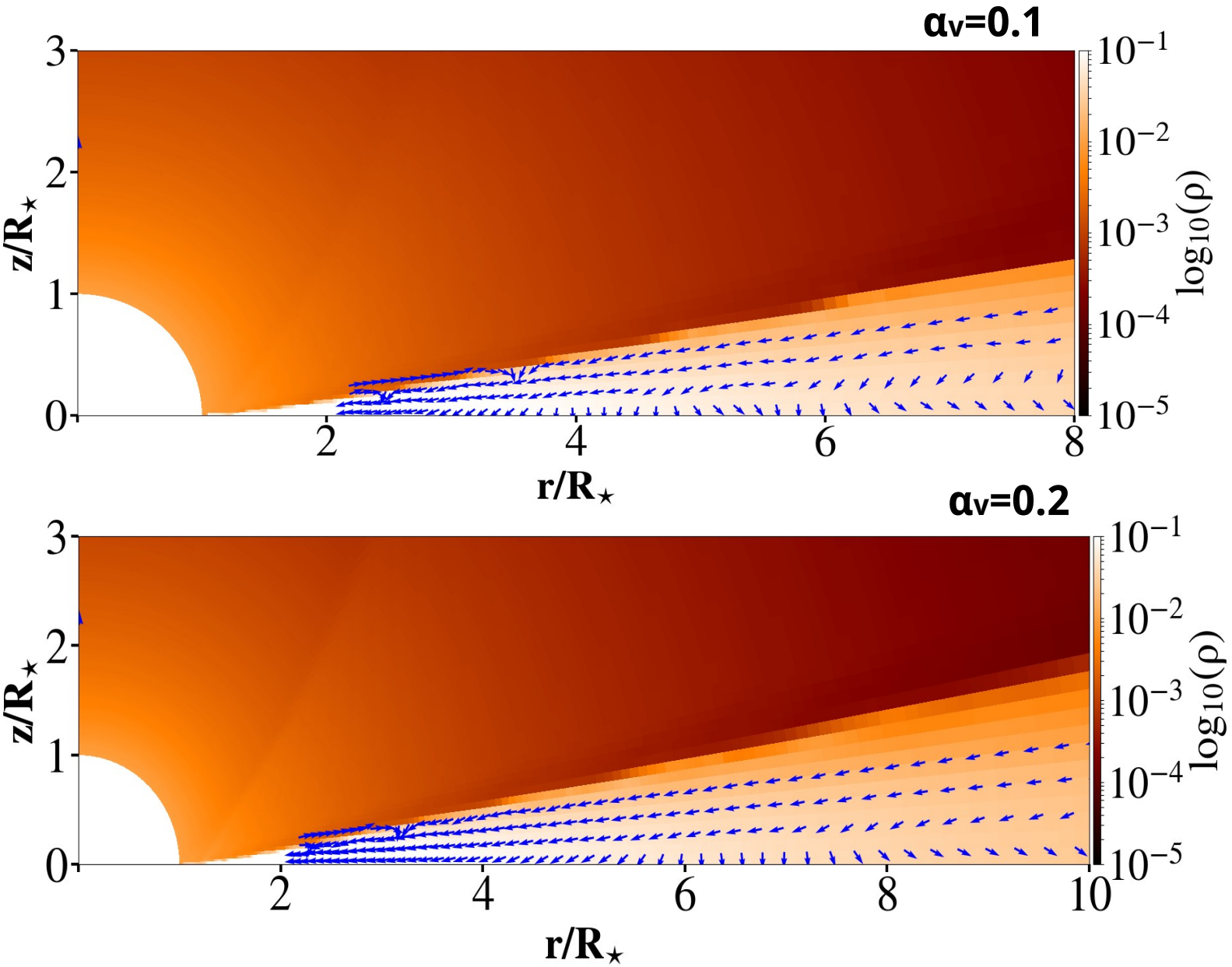

Backflows in the disk – HD case

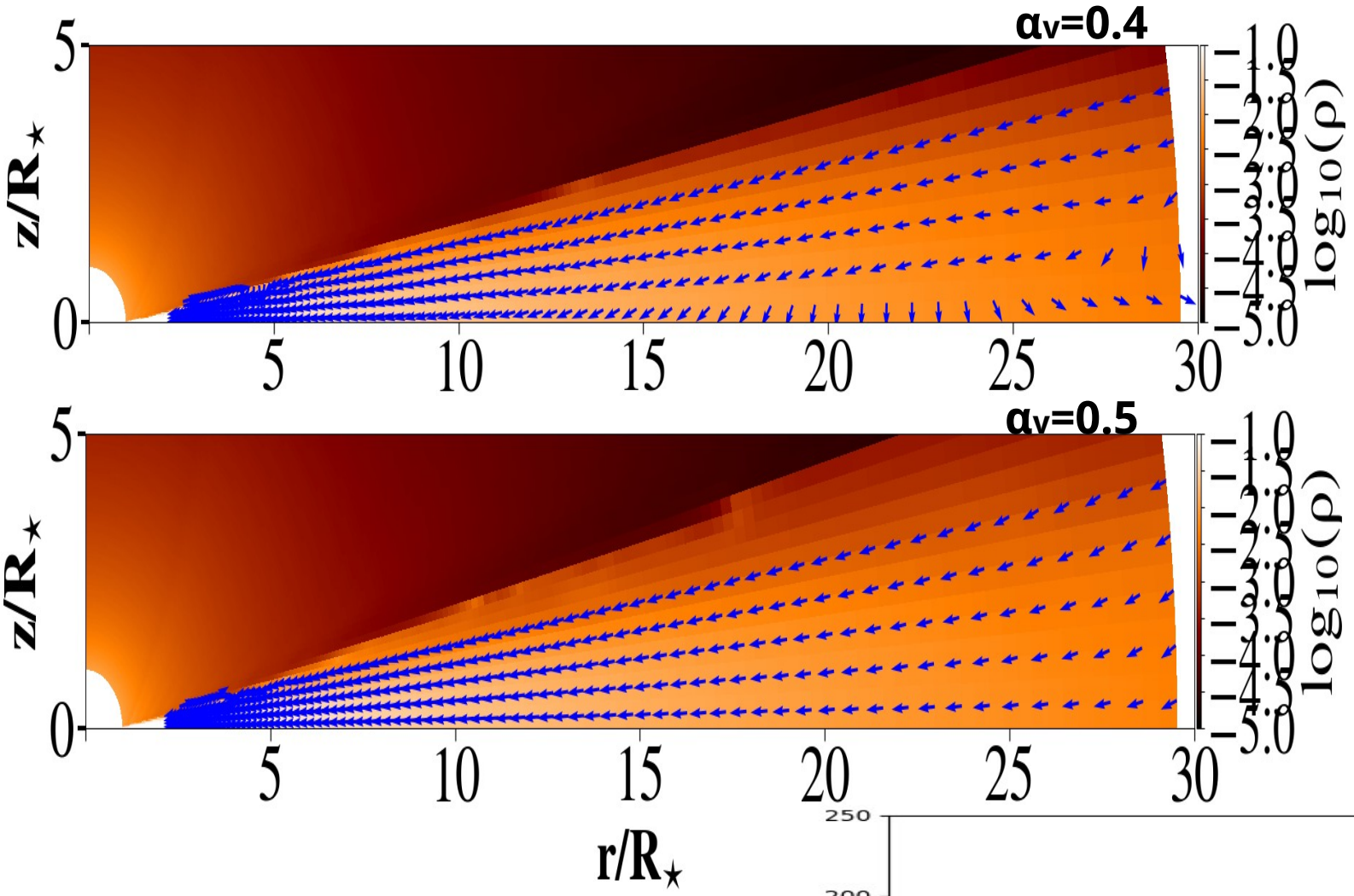

Ruchi took a look at the corresponding HD solutions, to check if the prediction from KK00 is followed also in the numerical simulations.

- Yes, it is.

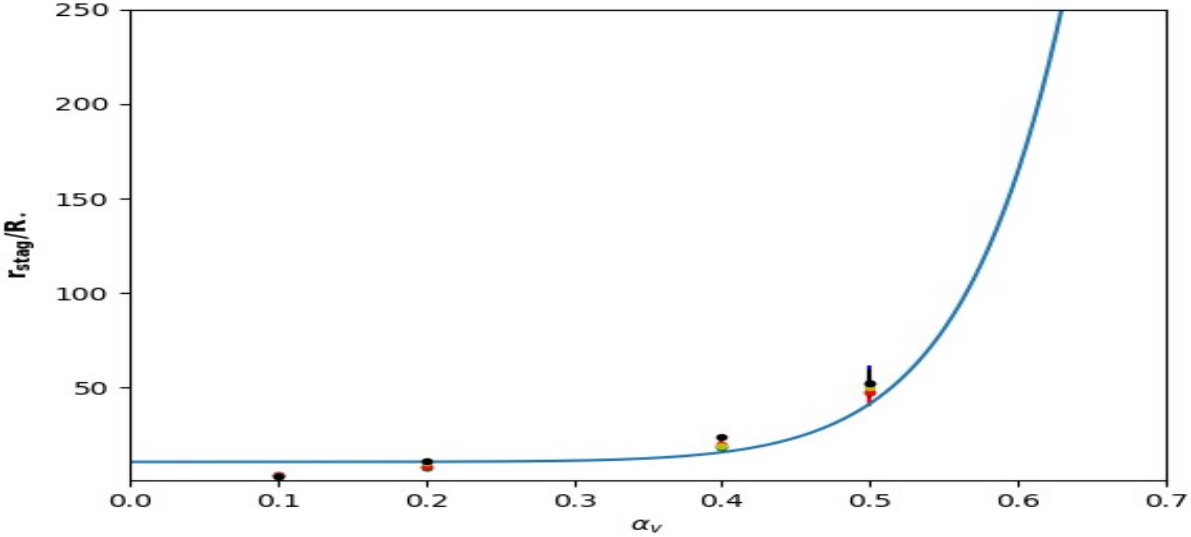

Backflows in the disk – MHD case

- How about the MHD case? Do we still obtain backflow in the disk? For which parameters?
- Here the answer is less clear, we are still trying to understand the results.

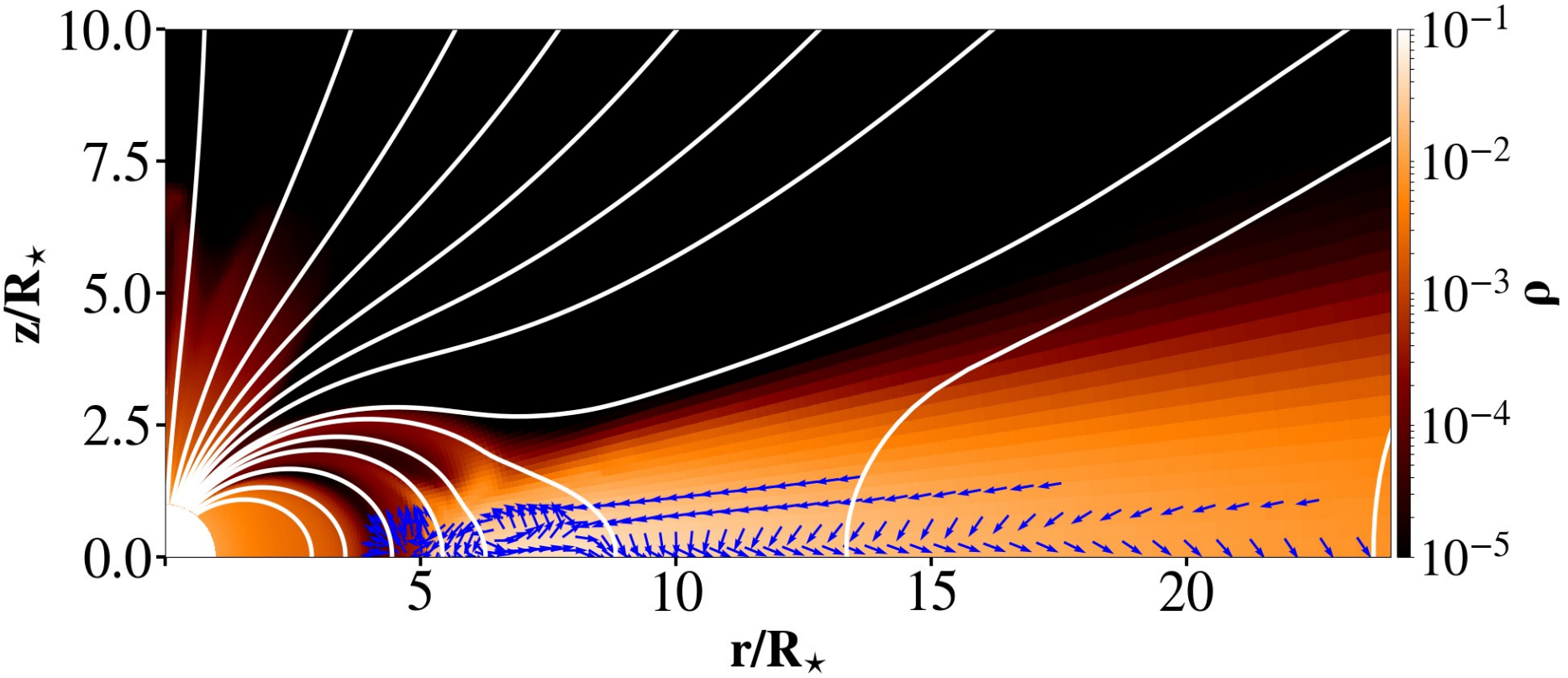

The jet launching

- In a part of the parameter space, there is a continuous launching of an axial jet from the star-disk magnetosphere. In my simulations, it showed that one has to wait until few hundreds of rotations of the star.
- The axial jet and the conical outflow are launched after the relaxation from the initial conditions. They are similar to the results in Romanova et al. (2009) and Zanni & Ferreira (2013).

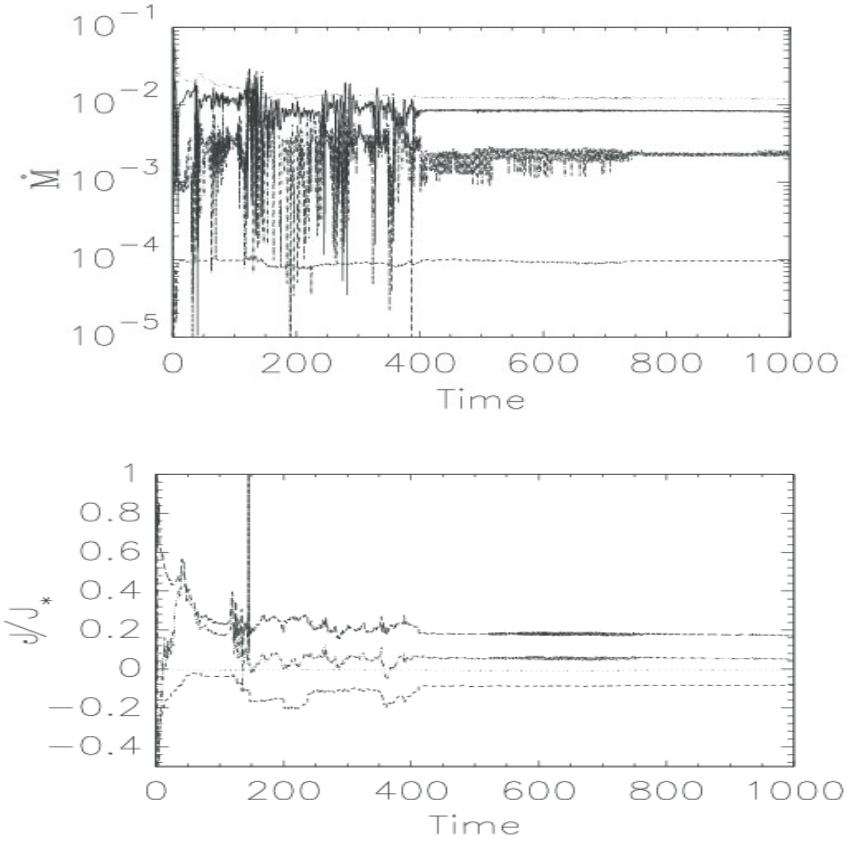

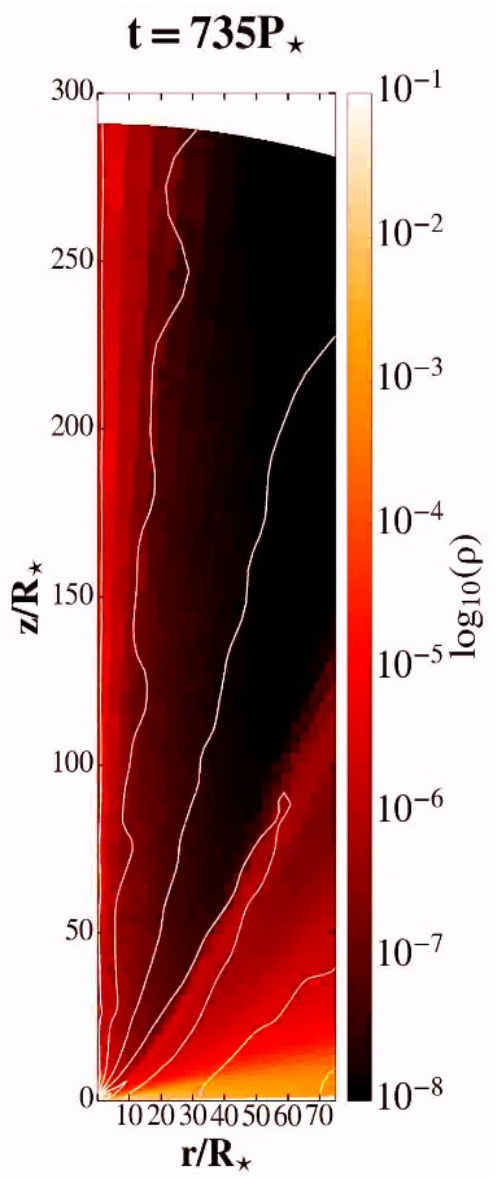

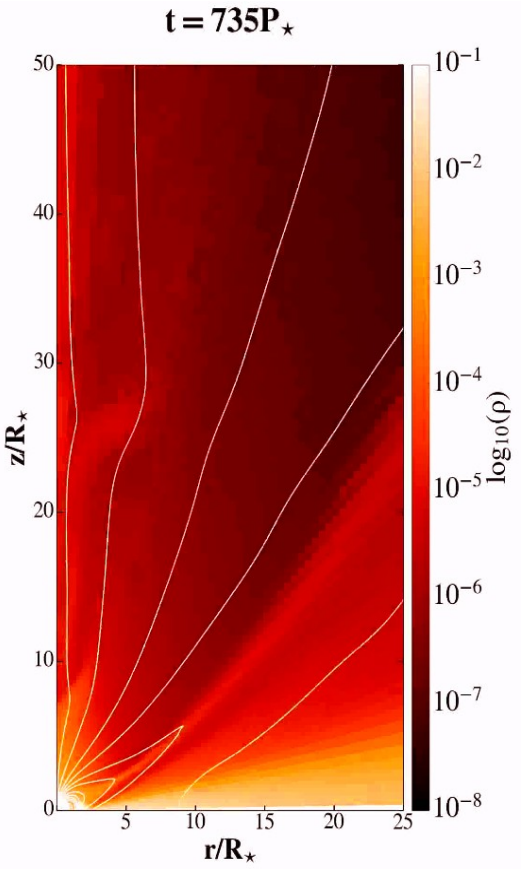

Zoom into the launching region.

Magnetospheric launching of conical outflow and axial jet

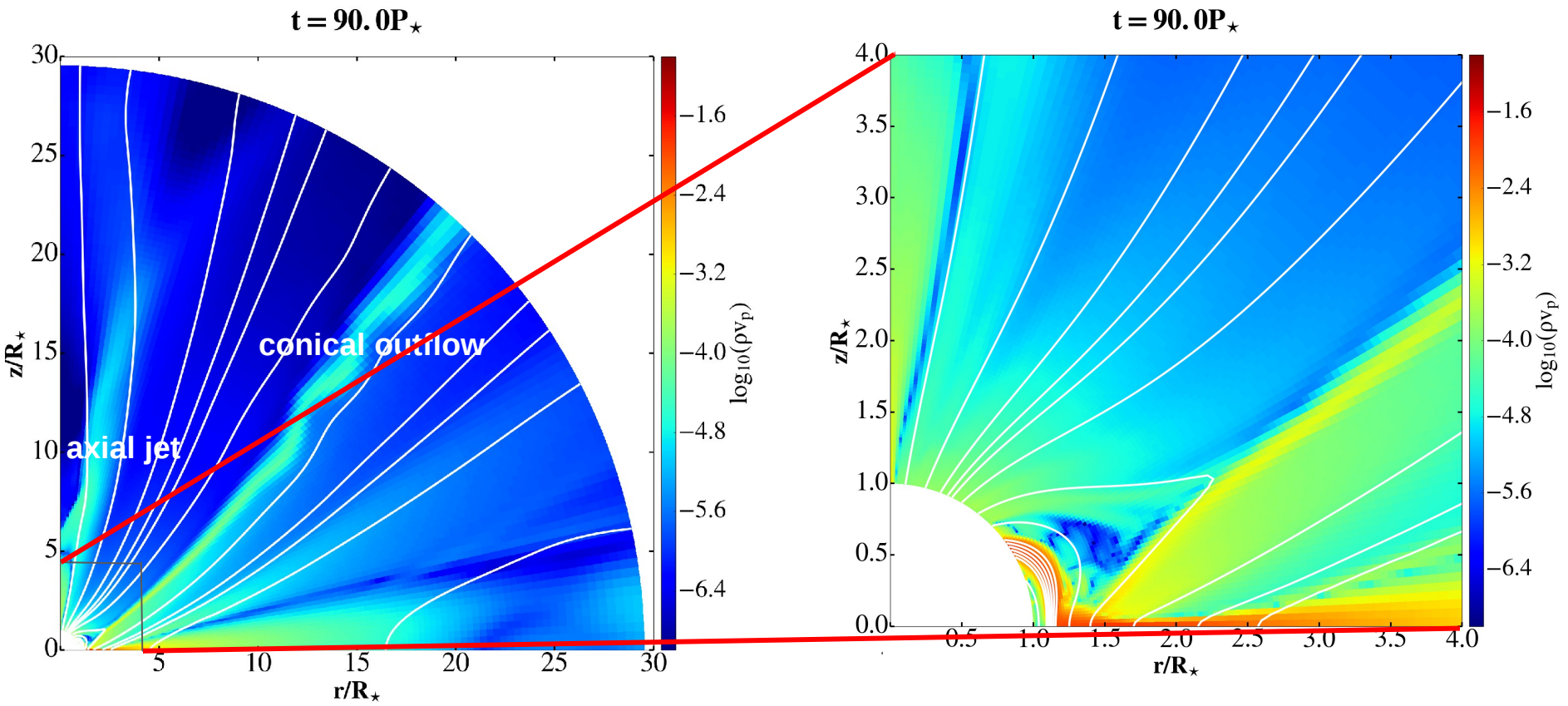

Color shows momentum in the MHD simulation in the young stellar object with conical outflow and axial jet, lines are the magnetic field lines. Right panel is a zoom into the left panel close to the star, to show the closest vicinity of the star.

The asymmetric jet launching (with A. Kotek)

With A. Kotek we took another look at the solutions with the jet launching: in the full meridional plane, with Rxϑ=[217x200] grid cells in ϑ=[0,π]. We obtain and analyze the asymmetric jets launched from the star-disk magnetosphere.

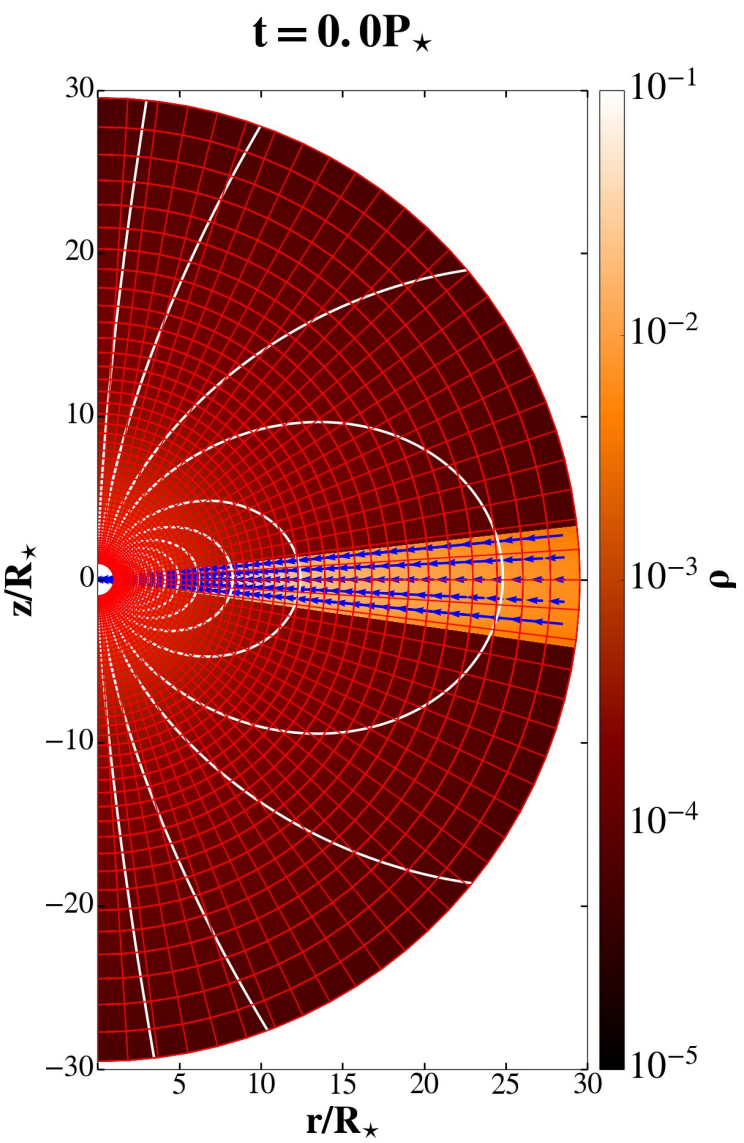

Initial setup in a full meridional plane.

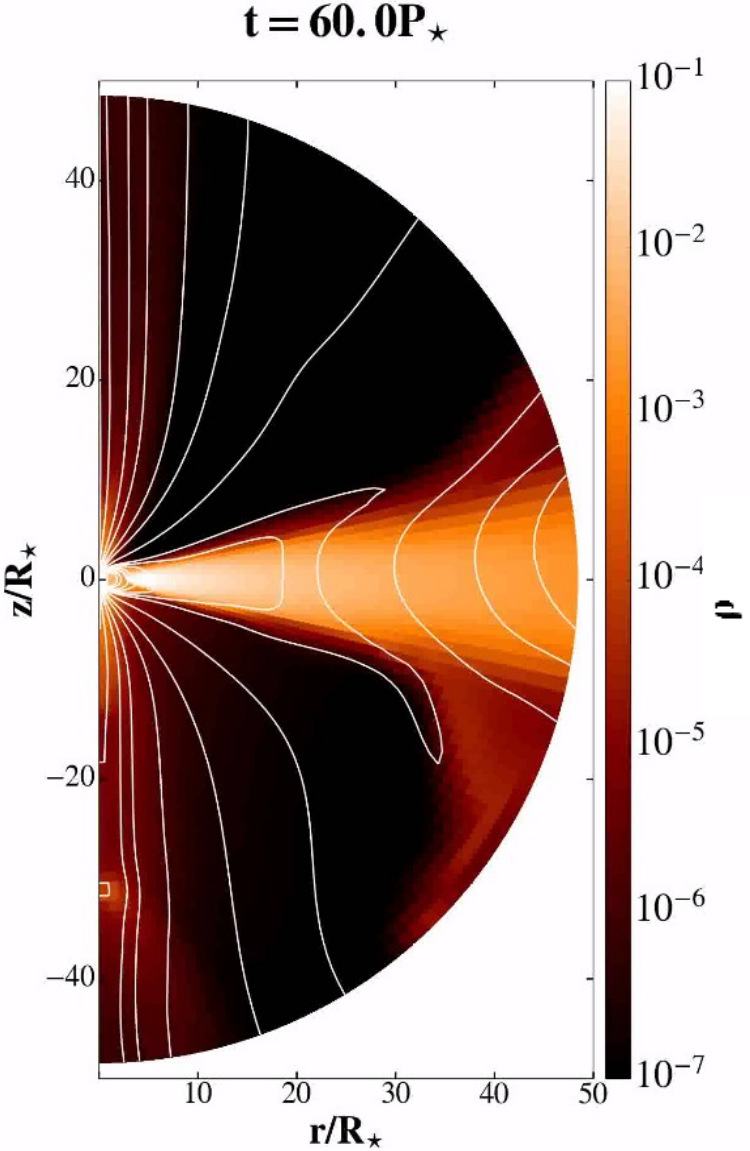

Asymmetric jet launched from the magnetosphere.

The asymmetric jet launching in 3D simulations

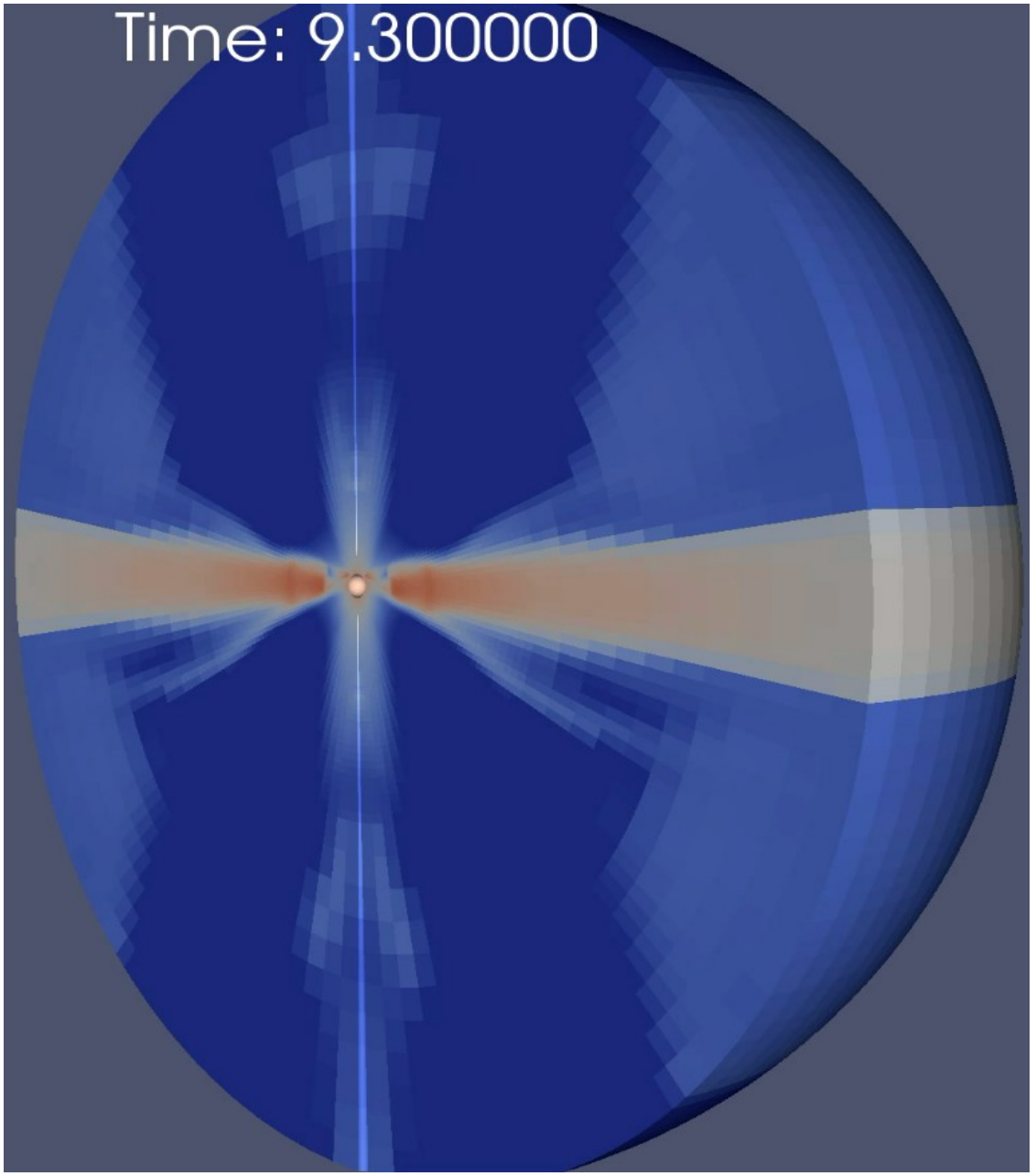

- In the full 3D simulations I also obtain asymmetric jets. To be continued... when, **and** if I find funding.

3D grid, Romanova et al.

- Ultimate goal of simulations work is to create a simulation which would produce the synthetic maps, which then could be compared with the observations.
- In simulations of magnetospheric star-disk interaction there is currently only one succesful setup in 3D: Romanova et al.
- Thanks to A. Koldoba's implementation of "cubed sphere" grid, this group produced, during the last 20 years, beautiful simulations with rotating star, disk and accretion column of matter from the disk onto a star.

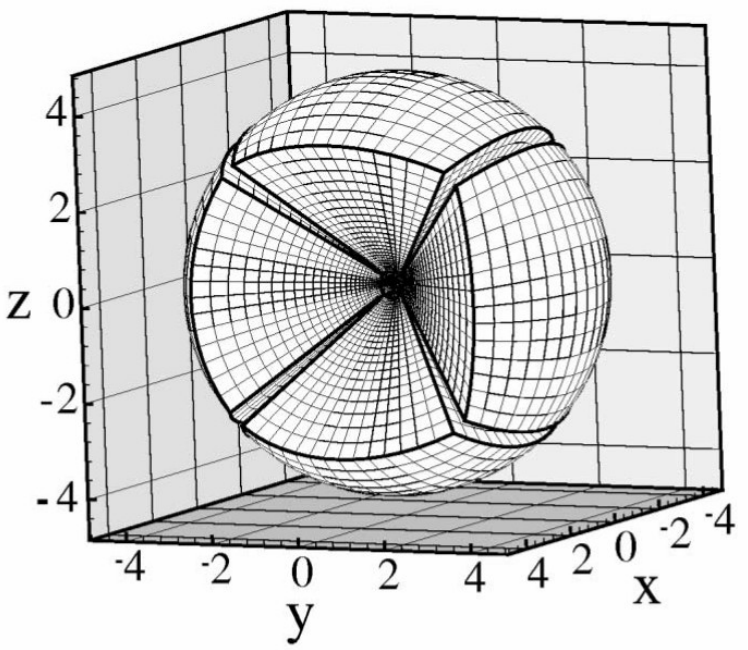

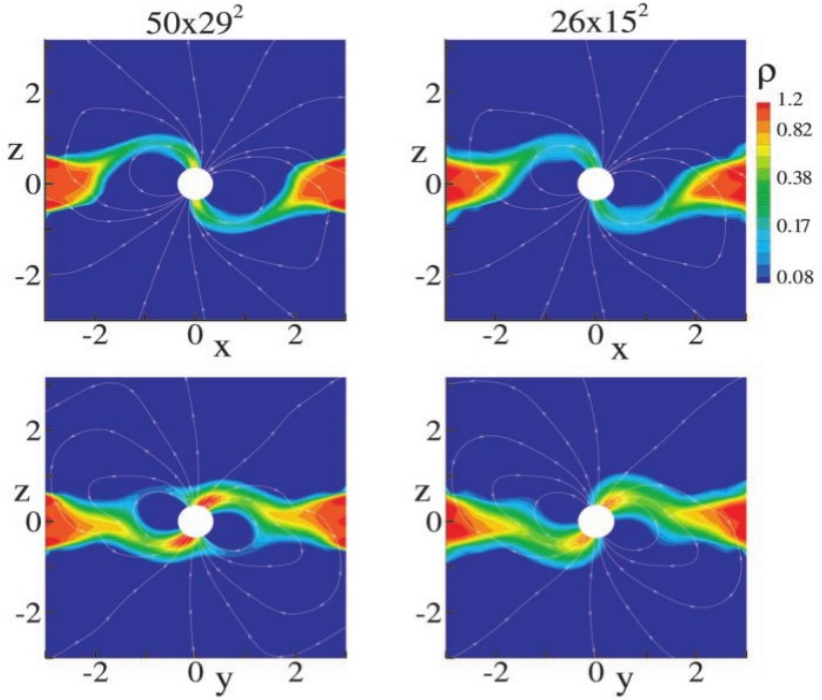

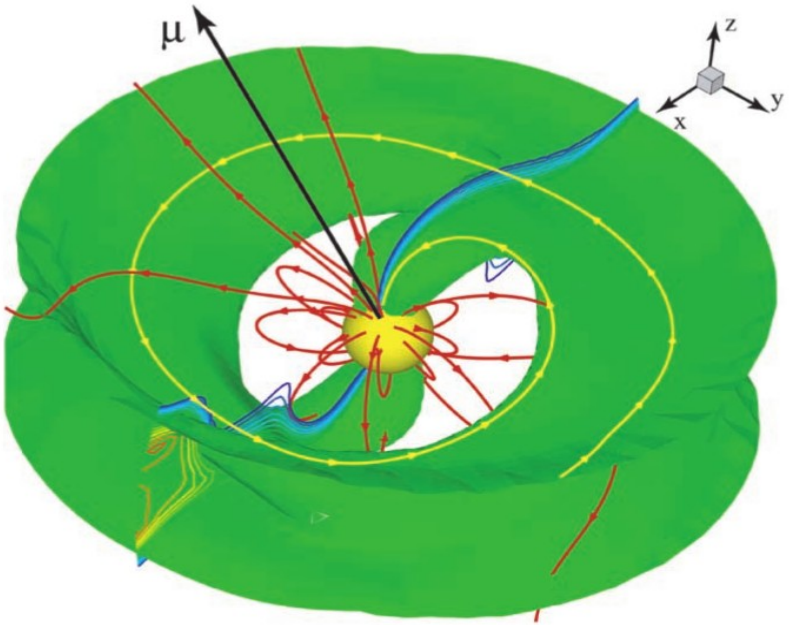

3D simulations, case with magnetic field aligned with rotation

- The first step here is to perform the axisymmetric 3D simulation. I use the spherical grid. The magnetic field in this case is aligned with the rotation axis.
- Zoom into the vicinity of the star=inner boundary condition at T=0 and at T=173

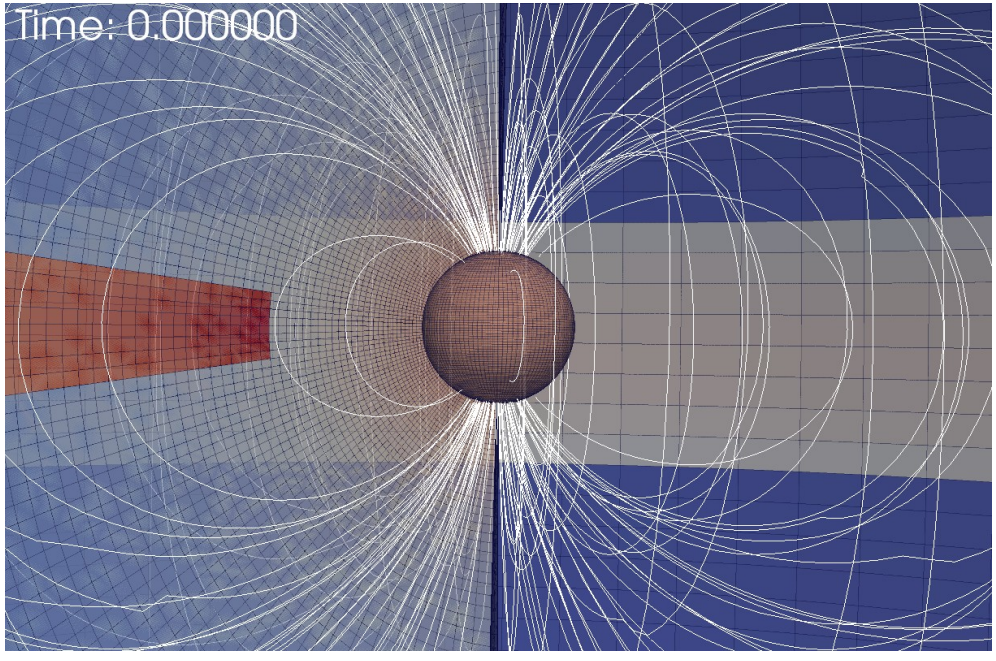

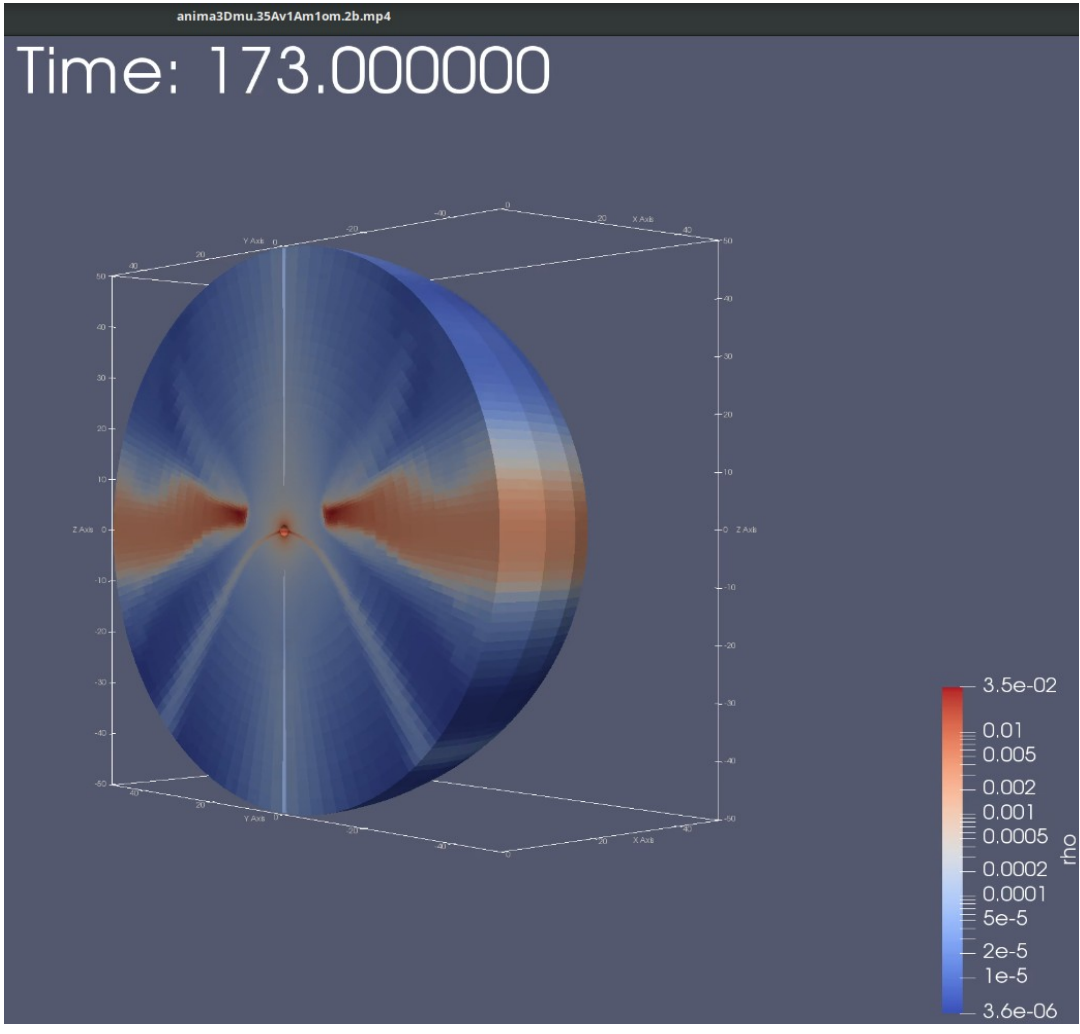

3D simulations, tilted magnetic field case

- The magnetic field in this case is not aligned with the rotation axis.

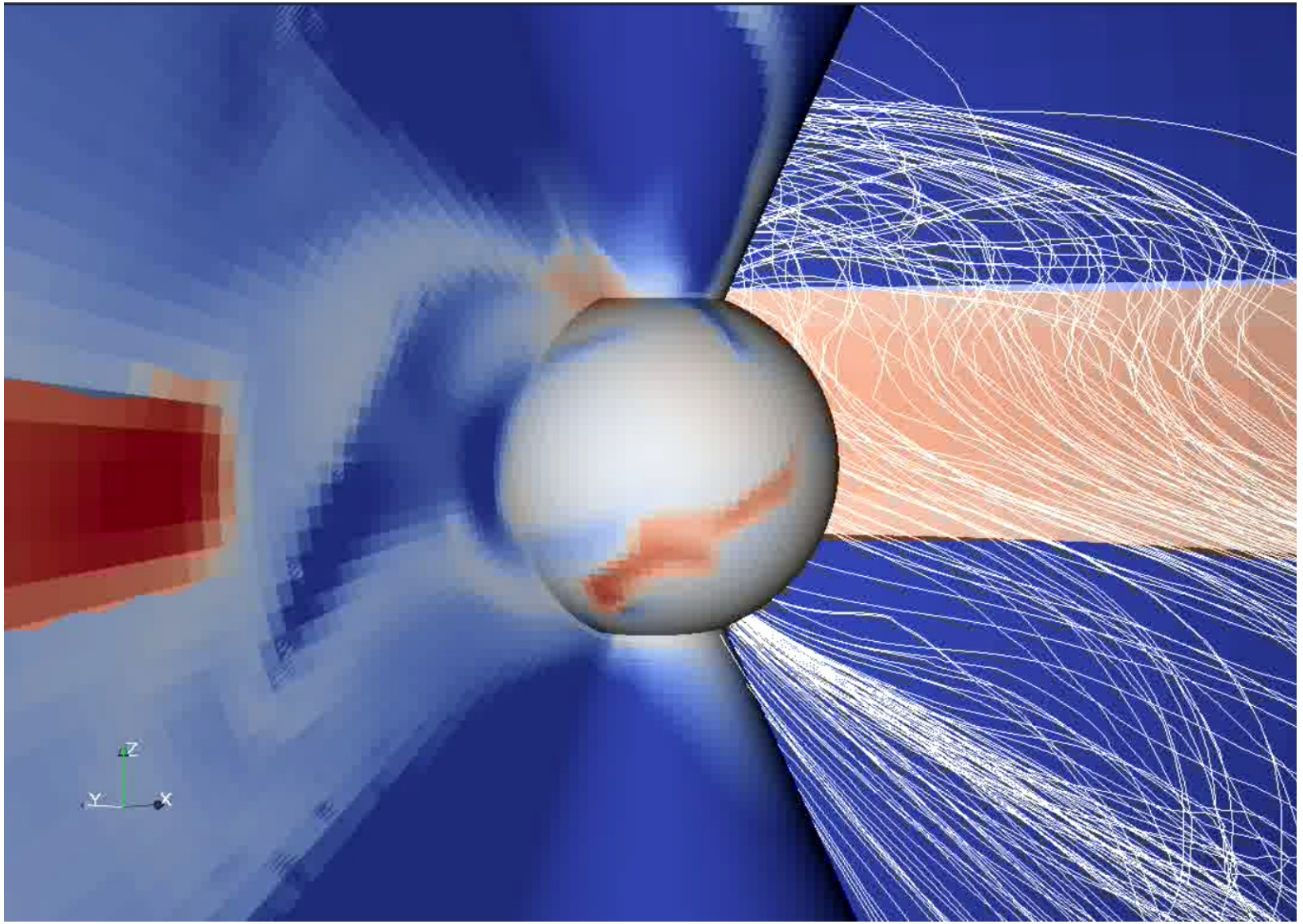

Connection to observations: 2D model for 3D light curve

The 3D simulations are tricky to obtain. Even if one does so, to make a parameter study is not straightforward. To use the 2D simulations with realistic parameters, I constructed a 3D model.

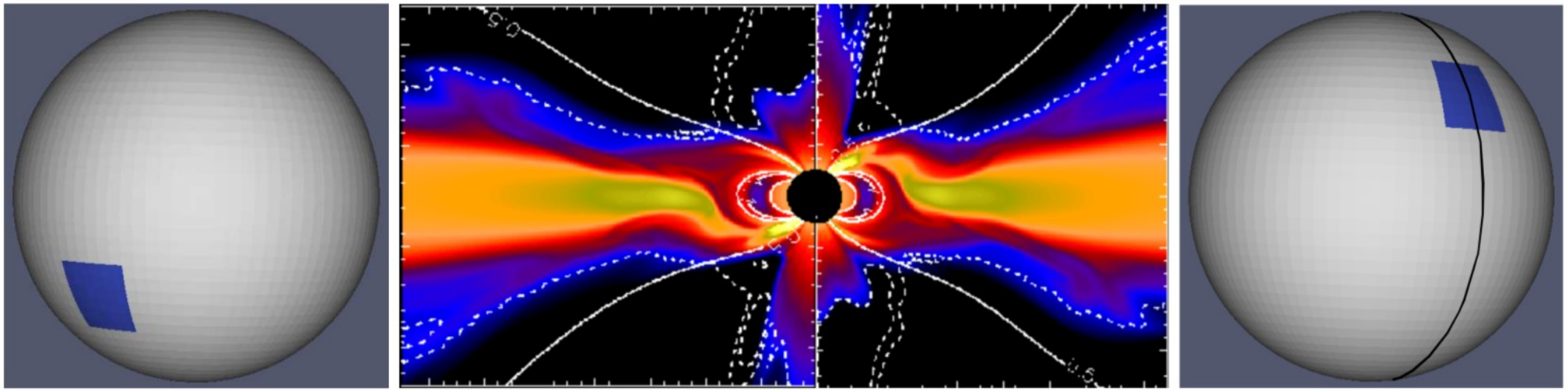

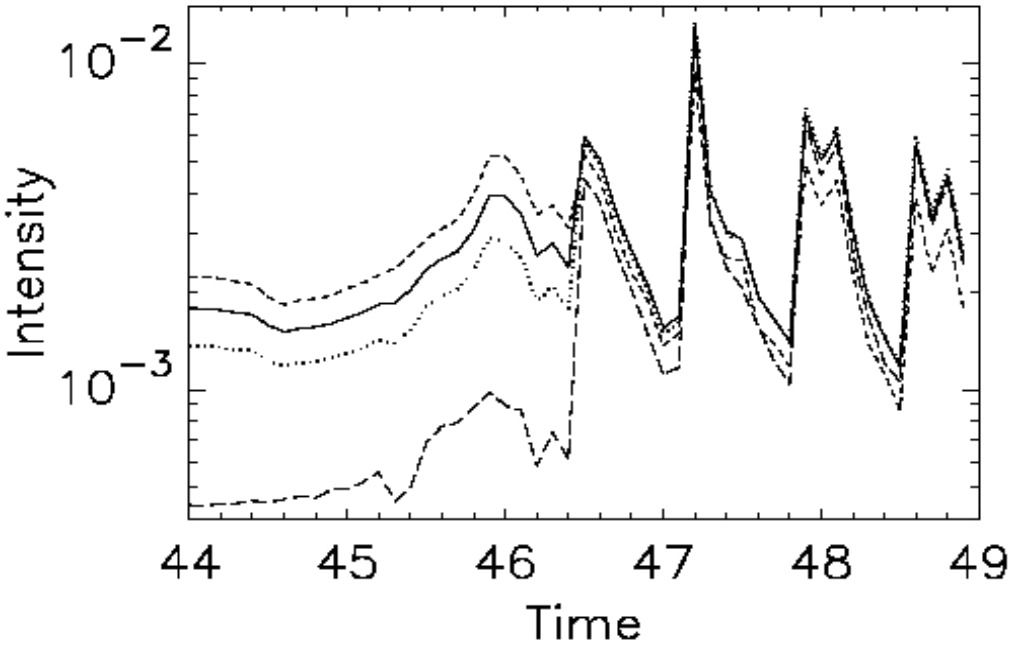

The emission integrated along the stellar rim one grid cell thick in the azimuthal direction. The solid, dotted, long-dashed and short-dashed lines represent the intensities for an observer positioned at a co-latitudinal angle θ =15, 30, 60 and 165 degrees, respectively.

Connection to observations: 2D model for 3D light curve
Bonus: the switching mechanism with the magnetic field aligned with the rotation axis

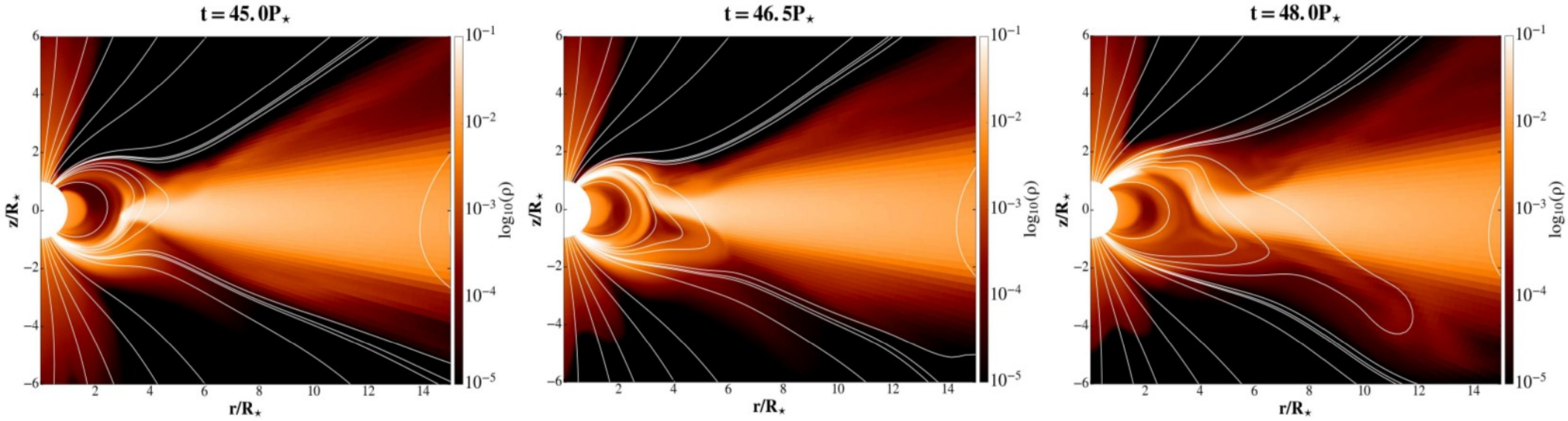

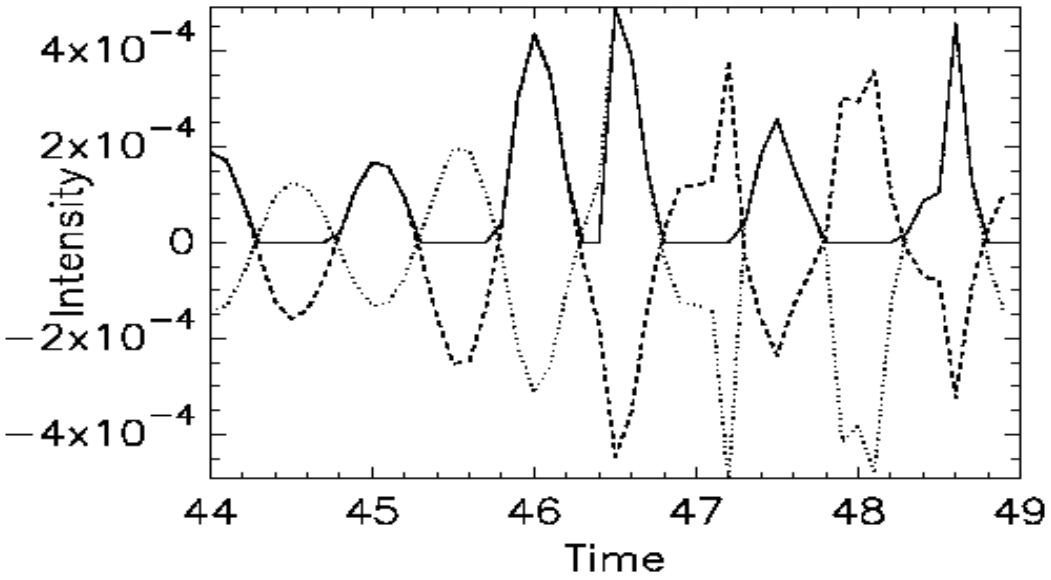

The dotted and dashed lines show the intensity for modeled hot spots as seen from the co-latitude angles of θ =15 and θ =165 degrees. Intensity is negative when the spot is not visible from a given position. In solid line is shown the total intensity for an observer with θ =165. Switching of the accretion column from the southern to northern hemisphere produces a phase shift in the observed intensity peak as the star rotates.

“STARDUST”: Dusty disk in Young Stellar Objects (with C. Turski)

In a Summer Program project C. Turski wrote the Python script “STARDUST” for post-processing of the quasi-stationary results in my star-disk solutions. He added the dust particles and computed their movement in the disk-corona solution as a background. The results are used to improve the model of dust distribution in the disk (with D. Vinković in a Croatian collaboration project “Stardust”).

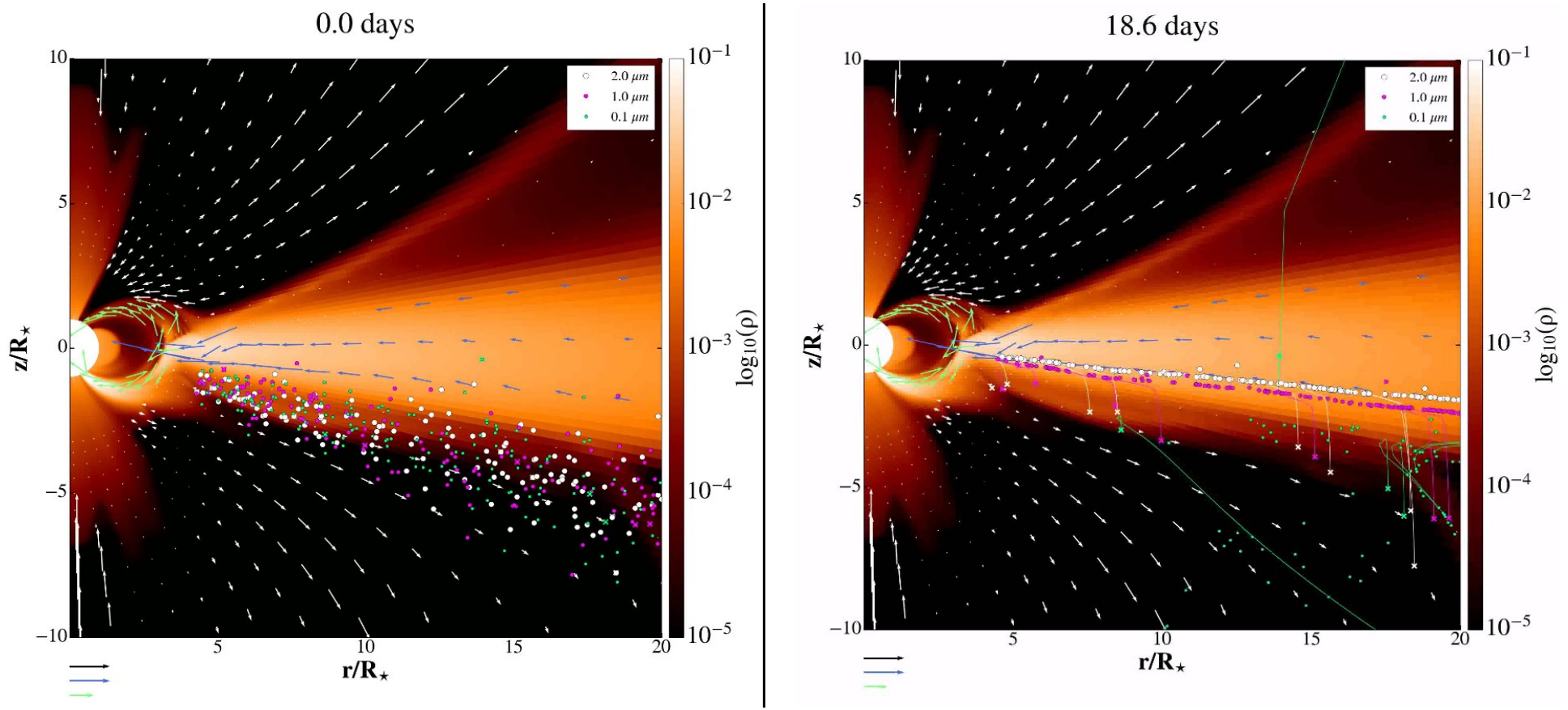

Summary

-I obtained viscous and resistive MHD star-disk magnetospheric interaction solutions for a thin accretion disk.

-A quasi-stationary state is obtained in a set of 64 simulations with slowly rotating stars.

-Results are compared, to find trends in solutions.

-In the cases with α_m=0.1, conical outflows are launched.

-We investigate results with backflows in the disk, in HD and MHD cases

-In the cases with faster rotating stars than those in our parameter study, axial jets are launched.

-We study in particular asymmetric axial jet launching.

-Currently, I am developing a 3D setup of star-disk simulations.

-To enable parameter studies, I constructed a 3D model from 2D simulations.

-As a bonus came the analysis of the switching of the column footpoint.

-Star-disk solutions are used as a background in a post-processing Python tool "STARDUST", to compute the trajectories of the dust particles of different sizes.